U.S. DEPARTMENT OF ENERGY | Office of Science

DOE/CM-TR-13-001
PNNL-22650

Improving the Characterization of Clouds, Aerosols and the Cryosphere in Climate Models

Philip Jones
Los Alamos National Laboratory

Philip Rasch
Pacific Northwest National Laboratory

Stephen Klein
Lawrence Livermore National Laboratory

Progress Report 2012
December 17, 2012

DISCLAIMER

This report was prepared as an account of work sponsored by the U.S. Government. Neither the United States nor any agency thereof, nor any of their employees, makes any warranty, express or implied, or assumes any legal liability or responsibility for the accuracy, completeness, or usefulness of any information, apparatus, product, or process disclosed, or represents that its use would not infringe privately owned rights. Reference herein to any specific commercial product, process, or service by trade name, trademark, manufacturer, or otherwise, does not necessarily constitute or imply its endorsement, recommendation, or favoring by the U.S. Government or any agency thereof. The views and opinions of authors expressed herein do not necessarily state or reflect those of the U.S. Government or any agency thereof.

Acronyms

AMT	Aerosol Modeling Testbed
ARM	Atmosphere Radiation Measurement program
BC	Black Carbon
CALIPSO	Cloud-Aerosol Lidar and Infrared Pathfinder Satellite Observations
CAM4	Community Atmosphere Model version 4
CAM5	Community Atmosphere Model version 5 (atm component of CESM)
CAPT	Cloud-Associated Parameterizations Testbed
CESM	Community Earth System Model
CICE	Los Alamos Sea Ice Model (ice component of CESM)
CLM	Community Land Model (land component of CESM)
COSP	CFMIP Observation Simulator Package
ENSO	El Niño and Southern Oscillation
FIE	First Indirect Effect
GCM	General Circulation Model
IARC	International Arctic Research Center
IN	Ice Nuclei
IPCC	Intergovernmental Panel on Climate Change
ISDAC	Indirect and Semi-Direct Aerosol Campaign
LANL	Los Alamos National Laboratory
LBL	Lawrence Berkeley Laboratory
LLNL	Lawrence Livermore National Laboratory
LWP	Liquid Water Path
MAM	Modal Aerosol Module
MERRA	Modern Era Retrospective-Analysis for Research and Applications
M-PACE	Mixed-Phase Arctic Cloud Experiment
NCAR	National Center for Atmospheric Research
NSA	North Slope of Alaska (ARM site)
OC	Organic Carbon
PNNL	Pacific Northwest National Laboratory
PNNL-MMF	PNNL Multi-scale Modeling Framework
POLMIP	POLARCAT Model Intercomparison Project
POM	Particulate Organic Matter
POP	Parallel Ocean Program (ocean component of CESM)
SCM	Single Column Model
SST	Sea Surface Temperature
UV-CDAT	Ultrascale Visualization, Climate Data Analysis Tool

WNP	Western North Pacific
WRF	Weather Research and Forecasting model
YOTC	Year of Tropical Convection

Contents

Figures

1.0 Introduction

The cryosphere, clouds, and aerosols are responsible for some of the strongest feedbacks in the climate system and are a large source of uncertainty in model-based assessments of climate change. In the Arctic, all of these elements combine to produce very rapid climate change. This project, entitled "Improving the Characteristics of Clouds, Aerosols and the Cryosphere in Climate Models," attempts a comprehensive and systematic study to improve the representations of these processes and to answer the question: What are the main processes driving rapid decreases in Arctic ice cover and what are the implications of those decreases on future climate? Researchers at the three partner laboratories are applying their broad expertise in these components to:

1. Improve model process representation of clouds, aerosols and the cryosphere,
2. Embed the improved representations into the Community Earth System Model (CESM), and
3. Assess the impact of those changes for simulations of past and future climate change.

For the Arctic, we are developing improved representations of sea ice strength and melt rates, aerosol deposition on snow/ice, Arctic clouds, Arctic biogeochemical feedbacks, as well as ocean circulation and permafrost hydrology. Improvements to global aerosol and cloud processes are also being undertaken because processes influencing aerosols and water vapor at lower latitudes affect Arctic aerosols, clouds, and the cryosphere.

This document describes progress for the 2012 fiscal year (FY) (October 2011-September 2012). Section topics are quite similar to last year's report. However, new work in those areas is described, and there is less emphasis on parameterization development and more emphasis on evaluation of the parameterizations and assessment of their impact. Over the remainder of the project, a larger fraction of the work will be devoted to integration and evaluation tasks, emphasizing implementation into the CESM and assessing the impact through hindcast simulations and climate change projections. Some activities within the project appear to be focusing outside of the polar regions, but as shown in a number of our studies, those processes also have an impact at high latitudes.

The following sections will describe progress in more detail, but highlights include:

- Implementation of multiphase ice and testing/preparation for release (Section 2.1),
- Improvement of aerosol deposition and resulting snowmelt (Section 2.2),
- Introduction of ecosystems into the sea ice model and first simulations (Section 2.3),
- Characterization of Arctic eddies and separation of time scales (Section 2.4),
- Quantification of the impact of ocean circulation on sea ice within CESM (Section 2.4),
- Development of tools to quantify and parameterize erosion and transport rates in permafrost regions to prepare for coupling with ocean (Section 2.5),
- Use of PNNL-MMF to inform and improve representation of high-latitude aerosols in CAM5 (Section 3.1.1),
- Exploration of aerosol sensitivity to emissions and transport pathways using different source inventories and regional tagging (Section 3.1.2),

- Study of monsoon impacts from local aerosol sources (Section 3.1.3),
- Development of prescribed-aerosol capability of CAM5 (Section 3.1.4),
- Addition of speciation for BC, POM, and dust in CAM5 (Section 3.1.5),
- Implementation of an intermediate modal aerosol model, MAM4 (Section 3.1.6),
- Assessment of impacts of previous changes to cloud microphysics and macrophysics (Section 3.2.1),
- Identification of two outstanding numerical issues that impact cloud physics, including unbounded PDFs and inconsistencies in time stepping/coupling of parameterizations (Section 3.2.1),
- Evaluation of CAM5 physics with a mesoscale WRF model to evaluate effects of resolution on clouds and aerosols in the Arctic (Section 3.3.1),
- Diagnosis of Arctic tropospheric stability bias due to underlying cold bias using CAPT configuration (Section 3.3.2),
- Assessment of Arctic cloud production using the CALIPSO observations (Section 3.3.3),
- Assessment of aerosol first indirect effect using ARM data (Section 3.3.4),
- Demonstration that the physically based parameterizations of Arctic low clouds in CAM5 are superior to those in CAM4 through a comparison of simulations to CALIPSO satellite observations using the CALIPSO simulator in CFMIP Observation Simulator Package (COSP) (Section 3.3.5),
- Implementation of a new ice nucleation scheme and an evaluation of satellite and ARM data (Section 3.3.6),
- Development of new tools and metrics to evaluate aerosol indirect effects (Section 3.3.7),
- Formation of new sub-teams to integrate and assess model improvements (Section 4).

2.0 Progress in Cryosphere Improvements

The work under this project spans many components and processes. Here, we describe our work to date on the cryosphere components, including sea ice, land ice, ocean, permafrost, and biogeochemistry within these components.

2.1 Sea Ice Multiphase Physics

Sea ice consists of a network of brine pockets surrounded by a matrix of fresh ice. The brine has a significant impact on the physical properties and biogeochemistry of the ice. The current version of the Los Alamos Sea Ice Model (CICE) has a fixed vertical salinity profile representative of multi-year ice. The aim of the multiphase portion of the project is to make the vertical profile of sea ice salinity a prognostic variable within CICE and to model the most significant processes that alter the salinity. We have been pursuing several approaches to address various, overlapping aspects of this problem.

The first approach includes a new vertical thermodynamic component for CICE based on mushy layer theory. In this framework, a continuum approximation is made where the network of brine pockets and surrounding ice matrix are averaged over a representative sample of sea ice. We use enthalpy and bulk

salinity as the prognostic variables, which are coupled through conservation equations. The coupled and non-linear nature of the resulting equations requires a different solution method to the one currently used by CICE. We use a Jacobian-free Newton-Krylov method to solve the system. The system of equations requires the liquidus equation for seawater. We have implemented one based on experimental data that is more accurate than any currently deployed in a sea ice model.

One of the most important processes that change the salinity profile of the ice is gravity drainage. When sea ice forms, the upper layers are colder, and so contain denser brine, than deeper layers. This unstable density profile results in the brine draining out of the ice that will be replaced by fresher seawater, causing a significant desalination of the ice. Using time-resolved observations of bulk salinity and temperature of forming sea ice (Notz and Worster, 2008), we have shown that desalination proceeds as two distinct modes: rapid drainage at the base of the ice and slow drainage occurring more deeply in the ice (Turner et al. 2012). We have implemented a parameterization of these two modes of gravity drainage within the new thermodynamic component, and model results reasonably reproduce the observational data. Figure 2.1 shows a comparison between the time-resolved observational data and model output using the above gravity drainage parameterization for forming sea ice in Adventfjorden, Svalbard. Observations take place at set depths within the ice: dark blue colors correspond to sensors near the top surface of the ice. The bottom two panels show bulk salinity and the two modes of gravity drainage are visible.

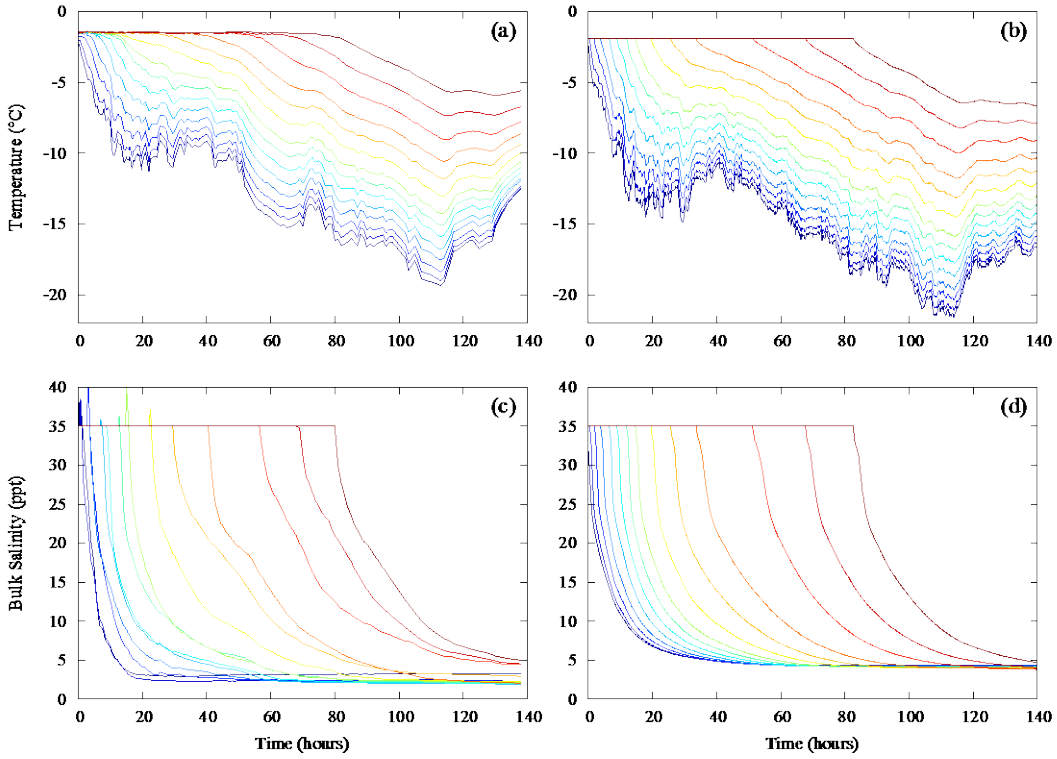

Figure 2.1. Temperature (°C) versus time (hours) for (a) the individual wire pairs in field observations, and (b) the corresponding model simulation with 100 layers. Bulk salinity (ppt) versus time (hours) for (c) the individual wire pairs in field observations, and (d) the corresponding model simulation with 100 layers. Model data is interpolated to the same depths as the wire pairs in the experiment.

Other processes alter the salinity profile of sea ice. Summer melt water percolates through the network of brine channels, resulting in further desalination. This process has been implemented in the new thermodynamic component, where a hydraulic head in a melt pond forces a Darcy flow of melt water downwards, which desalinates the ice to very low bulk salinities. Interestingly, this does not significantly decrease the porosity. This is in contrast to observations that show the formation of "interposed" ice during this flow, which blocks channels and makes the ice impermeable. The accurate representation of melt ponds requires an accurate modeling of their drainage through the ice so further work will be undertaken to determine why interposed ice does not form in the model.

Unlike the Arctic, a significant amount of new sea ice forms in the Antarctic through flooding of snow by seawater. In the Antarctic, it is common for enough snow to accumulate on sea ice to depress the snow-ice interface below sea level. Seawater then floods the lower levels of the snow, and over time it freezes to form sea ice. In the current version of CICE, this process occurs by the compaction of snow to form ice, thus bringing the snow-ice interface back above sea level. In the new thermodynamic component, the upward flow of brine though the porous sea ice and the amount of flooded snow are explicitly calculated. Flooded snow is not compacted but added to the ice layer with an appropriate porosity and salt content. The newly formed ice then undergoes gravity drainage, as previously described. If the sea ice is impermeable, flooding will not occur. However, the negative seaboards for the snow-ice interface will occur, as is observed in Antarctica.

A second approach addresses the vertical transport of salt and nutrients through the brine channels and is suitable for broader modeling applications. It contains elements of the mushy layer theory for salinity but also applies to passive tracers, like CO_2 and black carbon. Transport of salt is more complicated than that of other inclusions; salt alters the brine channel structure of the sea ice during transport. Jeffery et al. (2011) demonstrate that internal passive tracer motion induced by gravity drainage could be modeled using a tracer-velocity dispersion coefficient. However, the dispersion coefficient is a function of the vertically resolved, dynamic sea ice salinity.

During the course of this project, we have developed a model of sea ice salinity in two-way thermodynamic coupling with CICE. The prognostic salinity scheme is based on the theory of multiphase passive tracer transport, and it incorporates the gravity drainage dispersion coefficient of Jeffery et al. (2011). Melt water flushing is included as advective Darcy flow with explicit solution of the hydraulic pressure head. Both the brine surface height and isostatic adjustments of the ice column determine the pressure head that governs the strength and direction of the flow. In this way, surface melt water accumulation forces a downward percolation of brine, while snow accumulation and high basal melt naturally lead to an upward brine migration. Both processes have been observed in the field and are essential components of a predictive global sea ice model.

In Jeffery et al. (2012), we present the first Arctic -wide simulations of 3D sea ice halo-thermodynamics with full inclusion of CICE elastic-viscous-plastic dynamics, advection, and ridging. Arctic simulations, in contrast with the original fixed salinity version of CICE, show reduced spring melt, greater minimum ice extents, increased ice thickness, and a reduced seasonal cycle in ice volume. In addition, the model captures the characteristic features of observed salinity profiles after a decade of simulation from two sampled regions in the Arctic with distinct ice types. In Figure 2.2, we show contours of simulated Arctic salinity during the 1990 sea ice maximum and minimum extent. Observations of extent match the modeled ice edge quite well.

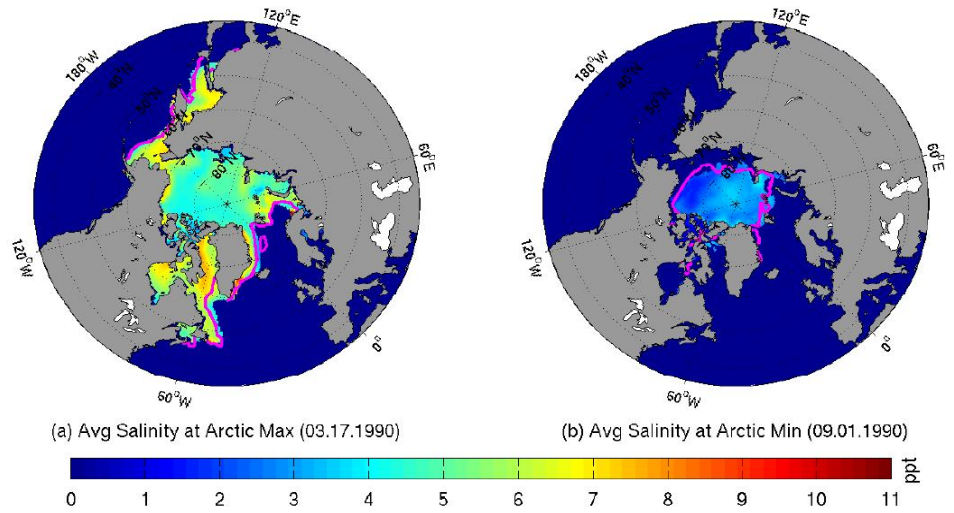

Figure 2.2. Depth averaged Arctic sea ice salinity during (a) maximum and (b) minimum ice extent. Fuchsia contours are satellite-derived monthly mean ice extents for March and September, 1990 (Cavalieri et al. 1996).

Currently, motions of the brine surface only arise from local melt and permeability conditions. A brine surface above the ice level is a local melt pond, and its height and salinity are predicted by our model. In the Arctic, horizontal processes, such as flow over uneven surface topography or along permeable ice layers, are very important in modeling realistic melt ponds. Work is ongoing to couple the melt pond parameterizations recently incorporated into CICE, with the salinity and brine surface information computed by the prognostic salinity scheme.

A third part of the sea ice salinity effort involves the surface melt pond parameterizations. Sea ice volume is highly sensitive to the thermodynamic fluxes that determine the surface energy balance, of which shortwave and longwave radiation are critical components in summer. Summer melt ponds, pools of melted snow and ice that collect in depressions on the ice surface, are relatively dark in color and can lower the surface albedo considerably from the relatively high values associated with snow cover and bare ice. The surface albedo continues to decrease as more melt water collects on the ice, increasing solar absorption and further melting the ice and snow, an important albedo feedback process. The formation, evolution, and disappearance of melt ponds are governed by complex processes, including interactions with the existing snow layer, drainage rates through permeable sea ice, episodic refreezing, and considerations of ice topography

Two new melt pond parameterizations have recently been incorporated and tested in the CICE model. The first one ("topo ponds"), developed by collaborators at University College London, uses the simulated ice thickness distribution as a proxy for the ice topography to determine the areal extent of ponds on top of sea ice; liquid water drains onto the thinnest ice in each grid cell. The second parameterization ("level-ice ponds"), developed at Los Alamos (Hunke et al. 2012) uses the sea ice ridging diagnostics now available in the model; ponds drain from ridged ice and collect on undeformed, level ice. For both parameterizations, realistic model hindcast simulations are used to explore the interactions of physical mechanisms that affect the evolution of ponds and sea ice albedo, and the results are compared with Arctic *in situ* measurements and satellite-derived observations (Flocco et al. 2012).

Melt ponds first appear at southerly latitudes in spring, moving north as the melt season progresses (Figure 2.3). Ponds form quickly and initially are widespread, then pool into low topographic features and begin to drain through permeable ice within a few weeks. The pond area then slowly increases due to continuing snow and ice melt until the ponds' upper surfaces begin to refreeze. Because of variations in topography and permeability, we find deeper ponds on thicker, more deformed ice, and these are the last to freeze over in autumn. Sensitivity tests reveal that the snow simulation is critical, because the volume of snow deposition and rate of snowmelt largely determine the timing and extent of the simulated melt ponds.

In the level-ice pond study, we discovered a level-ice-pond feedback mechanism that has not been described previously, in which thinning ice has more level surface area available to be covered in ponds, enhancing thinning.

Finally, we have begun a collaboration with University of Colorado Boulder's Dr. Ute Herzfeld and her student, Brian McDonald, to investigate the sea ice ridging characteristics produced by CICE and compare them with *in situ* and aerial observations. We have created new diagnostics in the model, allowing us to compare the data and determine what factors are contributing to the resulting ridge distributions. At the same time, the observed data is being statistically analyzed in a form that is more comparable to model output. This is the first step needed to improve the ridging parameterization and processes controlled by it.

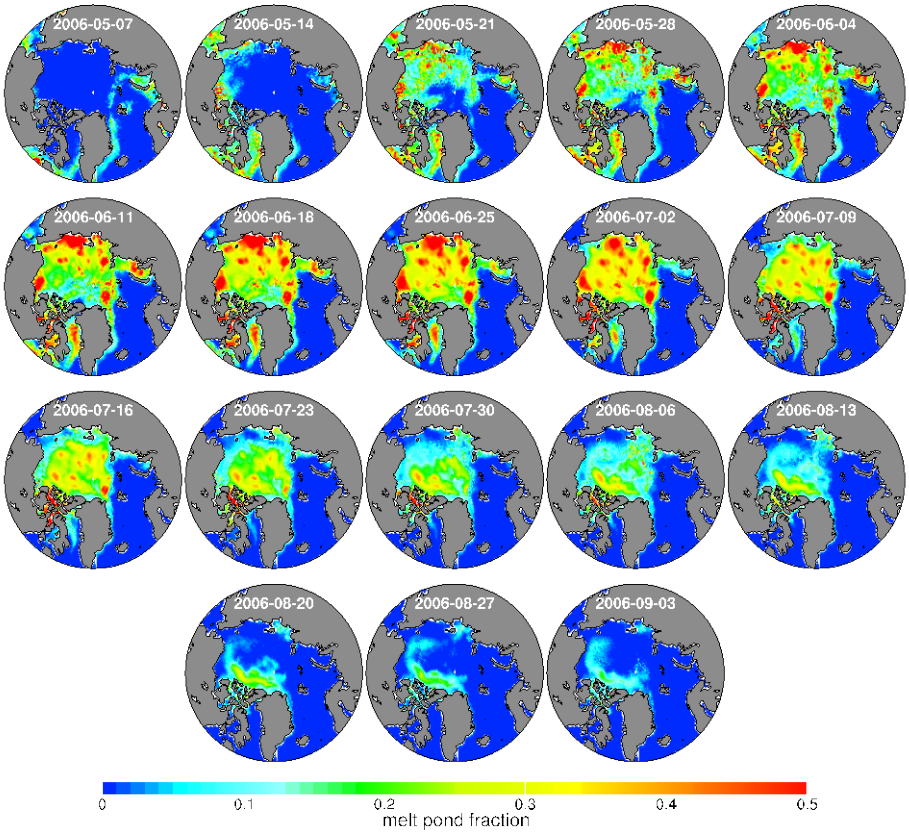

Figure 2.3. Ponded fraction of ice area, simulated for the Arctic in 2006.

2.2 Aerosol Deposition on Snow/Ice

In work described below (Wang et al. 2012a, submitted), we identified important sensitivities in Arctic aerosols to formulations of aerosol aging, convective transport and scavenging, and mid-to-high latitude scavenging in super-cooled liquid clouds. We developed CAM5 model parameterization revisions that produced substantial improvements in the fidelity of Arctic atmospheric aerosol simulations in both amplitude and seasonal cycle. The revisions increased aerosol (including light-absorbing BC and dust) deposition on snow and sea ice and modified the seasonal cycle of deposition, which has important implications for snow/ice melt and albedo change and their climate impacts. We have begun to modify CESM to use these deposition fluxes in the surface models discussed in Flanner et al. (2012). Figure 2.4 shows the changes in BC seasonal wet and dry deposition rate in modified simulations compared to the standard CAM5. Our PNNL team is collaborating with Mark Flanner (University of Michigan) and his postdoc to fully couple the SNICAR radiative transfer model to MAM aerosols in CAM5 to investigate the impact of increased absorbing aerosols on snow/ice melt and Arctic climate change.

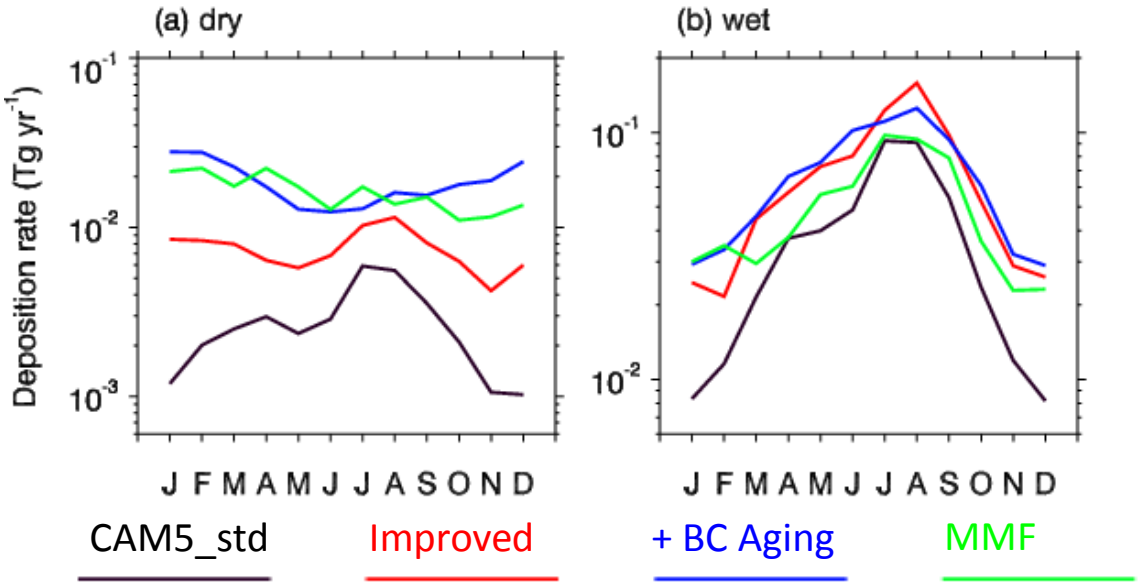

Figure 2.4. Seasonal cycle of (a) dry and (b) wet deposition rate in improved CAM5 simulations compared to standard CAM5 and MMF results (Wang et al. 2012b, in preparation).

2.3 Arctic Ecosystems

Over the past year, we have made significant progress in the development of ice algal and ice domain geocycling simulations. In particular, we report here results from work involving dynamic ice algal primary production, coupled open water to CICE trace gas chemistry, and release of aerosol precursors from the pack and surrounding leads.

Our primary production calculations began as a simple one-box representation published by collaborators at the International Arctic Research Center (IARC) in Fairbanks. We worked closely with IARC to introduce ice algal ecology and geocycling directly into the CICE code (Jin et al. 2012; Loose et al. 2011; Popova et al. 2012). This has yielded the community's first dynamic, Pan-Arctic computations of carbon fixation within the pack (Figure 2.5). The ice algal production calculations are necessarily

driven by nutrient inputs from below. Thus, they form a natural connection from standard global biogeochemistry of the Parallel Ocean Program to the full geochemistry that can be ultimately carried by CICE. Nutrients and organisms become the vehicle for a unique set of coupled seawater-to-ice simulations. For example, we have computed trends in carbon fixation over the decades prior to and including major coverage losses of the mid-noughts. Relative to the water column, our results are interactive in their treatment of nitrate/silicate inputs and return.

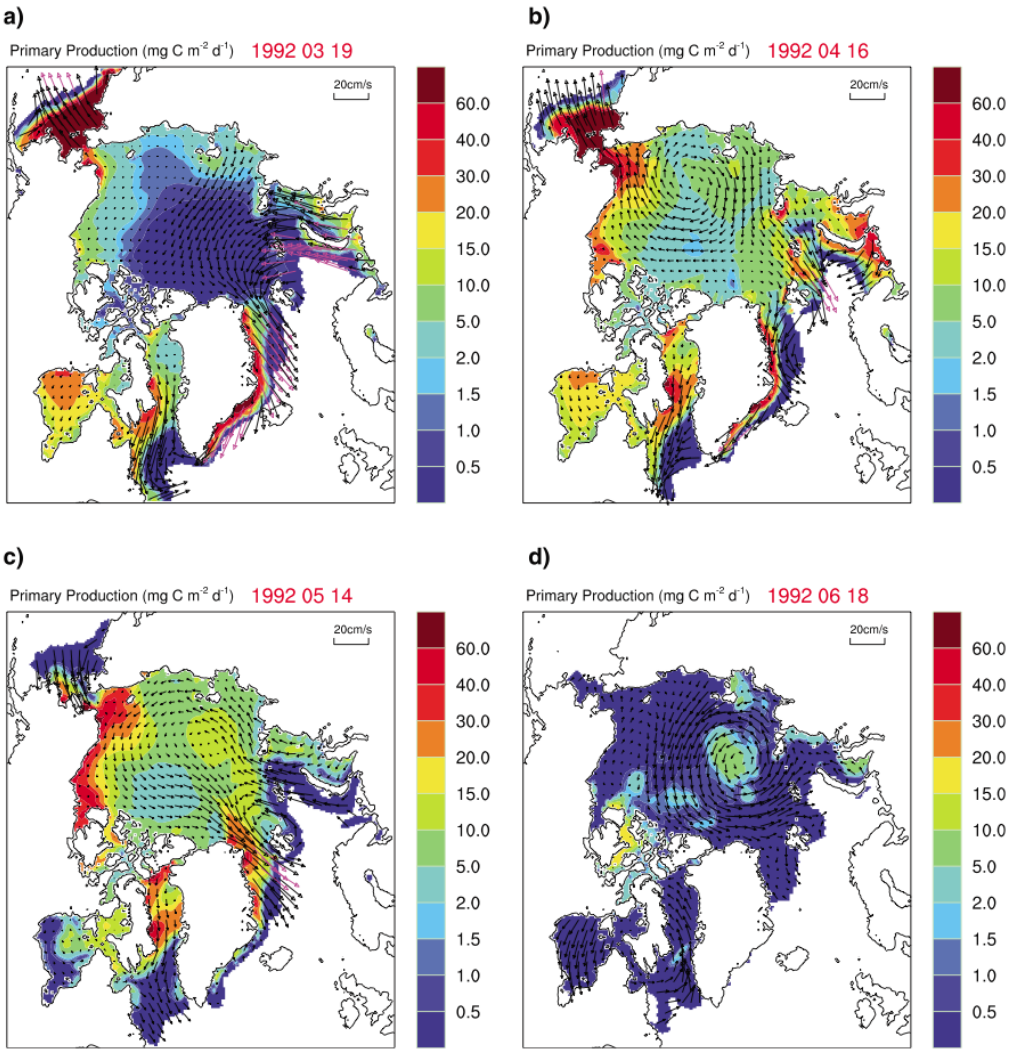

Figure 2.5. Primary production calculations demonstrating the development of an ice algal biogeochemistry simulator inside the dynamic CICE model. Carbon fixation as shown will drive the release or drawdown of CO_2 and availability of aerosol precursors to the atmosphere.

We also performed first-ever simulations of trace gas dynamics within a multi-dimensional ice model (Elliott et al. 2012; Humphries et al. 2012). In general, this work has focused on the reduced sulfur system, and more specifically, on the volatile aerosol precursor DMS. Our IARC colleagues are now extending the mechanism into an interactive POP-CICE framework, and they are performing a detailed analysis of the results. Indications are that releases from the ocean marginal domain will be strong, but highly sensitive to algal retention when confronted with spring freshwater purging.

A logical next step in the project will be to extend our computations from the realm of initial biomass generation to a complete carbon cycle of the pack. Even as photosynthesis removes dissolved carbonate from brine channels, exotic ice-specific minerals are forming and exerting their influence on pH (ikaite, vaterite). Ultimately this solid deposition process constrains CO_2 partial pressure and directs gas flow upward into the atmosphere. In the next year, we will introduce the low temperature, high salinity equilibrium constants required for a full calculation within the ice acid-base and solubility product systems.

An especially simple bridge to SciDAC macromolecular chemistry follows for ring ecosystems of the extreme Southern Ocean. The Antarctic sea ice domain is vast and tends to withhold dissolved iron, a crucial micronutrient. The polymers of life are intimately involved in this storage process. Frazil formation scavenges carbon chains from the winter water column, and they carry/imply high concentrations of metal binding ligands. Transition elements are therefore stripped simultaneously into the pack. Here, the coupling will be with our upcoming simulations of primary organic aerosol precursors. An objective will be to simulate the timing of trace metal return to open water moving into Antarctic spring and summer.

2.4 Ocean Circulation

The circulation in the Arctic is more uncertain than any other major basin owing to the lack of altimetry coverage at high latitudes, the difficulty of mounting polar observational campaigns, and the intricacy of the bathymetry. Coupled ocean-sea ice modeling has filled some of the gaps in our understanding of the basin but has also highlighted points where that understanding falls short. In this project, we have focused on high-latitude eddies and the impact of ocean heat transport on sea ice. Future work will explore Arctic halocline issues.

2.4.1 Characterization of Arctic Circulation and Eddies

The strongly eddying 0.1 degree global configuration of POP, used in a number of previous studies (Maltrud et al. 2008, 2010; Weijer et al. 2012), is now serving as the ocean component in coupled ocean-ice and fully coupled ocean-ice-atmosphere simulations (McClean et al. 2011). In the Arctic Ocean, where ocean stratification is weak and the effects of planetary rotation particularly strong, eddies are smaller than at midlatitudes. Our effort to characterize eddies is part of a broader effort to determine the degree to which the eddy field in the Arctic sector of our model remains limited by the present resolution and configuration of the model.

With colleagues funded under a separate visualization and analysis project (UV-CDAT), we have developed methods for identifying and characterizing eddy structures at high latitudes. These techniques, documented in a series of papers (Williams et al. 2011a, 2011b), have now been applied to the results from our high-resolution ocean simulations (Petersen et al. 2012). Eddy properties are shown here in Figure 2.6. We now intend to apply this same characterization to the analysis of POP regional Arctic simulations performed by Dr. Wieslaw Maslowski's group at the Naval Postgraduate School.

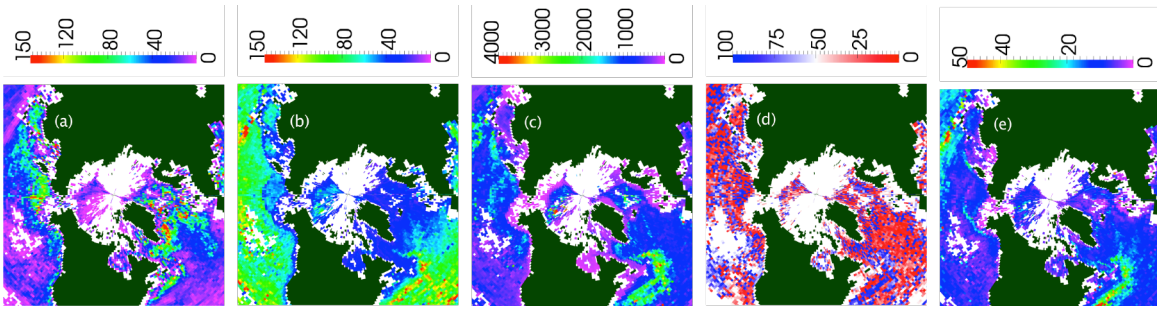

Figure 2.6. Eddy statistics from seven years of a POP ocean simulation: (a) eddy count; (b) diameter, in meters; (c) thickness, in meters; (d) percent cyclonic; and (e) eddy propagation speed, in cm/s.

2.4.2 Separation of Scales in Arctic Circulation

We have also been exploring the governing equations to identify unique characteristics of Arctic circulation, particularly the regimes of low stratification and relatively high rotation. In previous reports, the work of Wingate (2011) demonstrated a methodology to analyze a potential separation of scales in Arctic-like regimes. We are now using information derived from these analyses to develop new time integration methods for simulating ocean circulation, such as the design of physics-based preconditioners or new approaches, such as using fast-wave averaging or projection operators. We have created a relatively simple test problem and are implementing some potential schemes to evaluate the effectiveness of these approaches.

2.4.3 Sea Ice Response to Ocean Heat Transport

Ocean circulations and the associated heat transport have a strong influence on Arctic ice melt. Summertime Arctic sea ice has been decreasing at a remarkable rate in the later part of the 20th century. Various pathways associated with global warming have been proposed to explain this change, including changes in radiative fluxes due to greenhouse gases or aerosols, local feedback processes including cloud and sea ice albedo, and changes in heat transport by atmosphere and ocean circulations, but their relative importance remains uncertain. We used coupled CESM1 simulations to explore this issue with a particular focus on the role of ocean heat transport changes. Our study contrasted the role of different forcing agents in influencing ocean heat transport. We explored the role of ocean heat transport on CESM sea ice change and found this mechanism for delivery of heat to the Arctic is more strongly modulated by greenhouse gas forcing than by aerosols.

In Yoon et al. (2012a), we performed three ensemble simulations of the fully coupled CESM1 with CAM5.1 physics for the 20th century, forced by all forcing agents including GHGs, aerosol, solar, volcano, and land-use change. Based on these fully coupled CESM1 simulations, we further performed sets of slab ocean model (SOM) experiments to break down contributions from individual forcing terms: (a) GHG, (b) aerosol, and (c) ocean heat transport changes, and identified surface wind stress change due to increasing GHG is responsible for changes in ocean heat transport to the Arctic, especially over the North Atlantic Ocean. Figure 2.7 summarizes the results of SOM experiment showing the important role of ocean heat transport change in sea ice reduction.

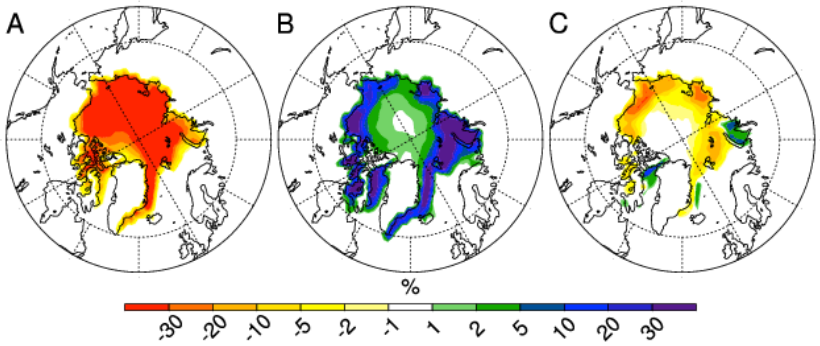

Figure 2.7. Change in the September Arctic Sea Ice cover (%) from early 20th century to late 20th century in CAM-SOM (GHG), CAM-SOM (aerosol), and CAM-SOM (ocean heat transport). GHG and aerosol can reproduce sea ice reduction with weaker intensity in the Atlantic and Bering Strait. With inclusion of ocean heat transport, sea ice reduction is stronger and matches with that of fully coupled CESM1. (From Yoon et al. 2012a).

2.5 Permafrost Hydrology

Since the last report, the focus of our permafrost hydrology efforts was to: 1) quantify hydrological characteristics and dynamics of Arctic rivers, deltas, and lakes; and 2) to identify the geochemical fluxes from Arctic rivers to the coastal ocean that have the greatest influence on coastal ocean geochemistry.

Completing the work started last year. Two manuscripts were finished regarding the natural variability of Arctic lake dynamics in Central Alaska (Chen et al. 2012a, 2012b). This research used remote sensing analysis of lakes over intra- and inter-annual time periods. The results will support better parameterization of Arctic lakes in CLM by quantitatively identifying natural (versus long-term warming) variability in lakes and statistically attributing observed changes to precipitation and evapotranspiration balances, river hydrology, and permafrost distributions.

Work is largely complete on developing a software program to analyze and quantify remote sensing output on river dynamics and characteristics. The program allows for spatial and temporal summaries of sediment fluxes due to river mobility and for fundamental characteristics such as river width and number of channels. The quantification of the sediment fluxes is critical to the incorporation of river fluxes to coastal oceans, allowing a quantification and parameterization of how changes in hydrological, water , and air temperatures will affect river dynamics in the Arctic.

In order to develop parameterizations for bank erosion that account for the relative influence of hydrological and thermal processes, an undergraduate student used two-dimensional process models of riverbank erosion to calculate erosion rates of riverbanks on two Alaskan rivers, assuming only hydrological processes controlled bank erosion. By comparing these modeled rates to observed rates in these systems with permafrost, the student was able to begin to quantify the relative influence of permafrost on the erosion rates. Another undergraduate student worked to extract hydrological data from remotely sensed images of deltas across the Arctic, including lake sizes, spatial patterns, and channel patterns. Because the physical structure of deltas control the transfer and storage of river-borne fluxes to the coastal ocean, these data will be used to develop a quantitative understanding of the role of deltas in modulating and altering fluxes from the landscape to the coastal ocean.

Finally, an effort is underway to quantify the influence of Arctic river discharges on coastal ocean geochemistry. For a set of six major Arctic rivers, a literature synthesis was conducted for a data of river fluxes of a suite of geochemical parameters (Fe, Si, Cu, TDN, DOC, P as PO_4, TDP, N as NO_3, N as NH_4, SiO_2, and SO_4). These data sets were run through a USGS software program to develop monthly loading estimates based on river discharge measurements. These data will be coupled to the ocean biogeochemistry model to determine what geochemical species have the most significant impact on ocean biogeochemical dynamics in the Arctic. Subsequent efforts to improve the river module in the land model, and the coupling of rivers to the ocean model, will initially be focused on the processes and dynamics that control these significant species.

3.0 Progress in Aerosol and Cloud Improvements

A second theme in this project is the exploration of a variety of cloud and aerosol processes that have strong impacts on polar climate and important climate systems near major aerosol sources. We completed and submitted papers documenting improvements that have been made to the representation of these processes in CAM5/CESM, and new capabilities to better understand aerosol and clouds in the climate system.

3.1 Aerosols

3.1.1 Improved Aerosols and Clouds in the Arctic

In our previous report, we described a variety of approaches toward understanding and improving the representation of aerosol, cloud, and transport processes in the CAM5/CESM model. These changes are described in Wang et al. (2012a). We used surface and aircraft measurements, together with a process-oriented and very costly multi-scale model (the PNNL-MMF), to provide insight into ways of improving the fidelity of CAM5 aerosols simulations and to evaluate the model improvements in predicting Arctic aerosols.

Our modifications to CAM5, targeted at improving the simulation of high-latitude aerosols, also improve aerosols globally over various regions, as shown by comparison of model-simulated aerosol optical properties to AERONET retrievals and mixing ratios to surface site measurements (e.g., IMPROVE, EMEP, University of Miami networks; Wang et al. 2012a). Moreover, a number of the modifications led to improvements in the climate simulation, such as an increase in CCN (shown in Figure 3.1), improved cloud droplet number

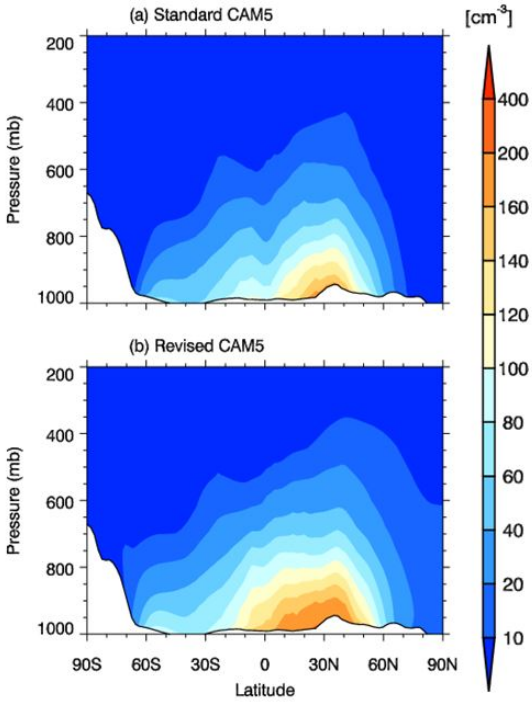

Figure 3.1. Zonal and annual mean number concentration of cloud condensation nuclei (CCN) (at 0.1% super-saturation) in the standard and revised CAM5 simulations.

concentration and liquid water path (LWP) (too low in the standard CAM5), and a relatively small decrease in precipitation rate. From the cloud microphysics point of view, increase in LWP and decrease in precipitation are generally consistent with the response of

clouds to increased atmospheric aerosol loading and the feedback of precipitation on cloud water. M. Wang et al. (2011) demonstrated LWP in CAM5 is more sensitive to anthropogenic aerosols than in MMF, leading to a stronger aerosol indirect forcing in CAM5. The magnitude of the LWP increases in our simulations is likely related to the strong response of cloud water to aerosol perturbations in CAM5. Some of our modifications reduced the fractional coverage of super-cooled liquid clouds but increased local LWP, caused by aerosol-cloud interactions and limiting the effect of the Wegener-Bergeron-Findeisen process, which is important in Arctic mixed-phase clouds. These changes in clouds have further impact on cloud forcings in the Arctic, which warrants further exploration into aerosol indirect effects in CAM5, including the impact of our new improvements.

We also compared simulations where CAM5 was constrained to agree with reanalysis products (ERA-Interim and MERRA) as an "offline model", comparing them to standard CAM5 simulations in which meteorological fields are internally determined ("free-running" simulations) to investigate the sensitivity in aerosol transport to general circulation patterns and eddy transport (Ma et al. 2012a). Our analyses suggest CAM5 is skillful in reproducing the important atmospheric circulation patterns that are responsible for aerosol transport to the Arctic, but some regional biases in meridional pressure gradients are observed in the free-running Community Atmosphere Model (CAM) Arctic oscillation (AO) pattern, resulting in stronger zonally distributed aerosols. This may have implications for Arctic aerosol source attribution and transport pathways.

3.1.2 Sensitivity of Arctic Aerosols to Emissions and Establishing Aerosol Source-receptor Relationships

In spite of the improvements by Wang et al. (2012a), a comparison of measurements suggests the model simulations still significantly under-predict surface-level BC and sulfate mixing ratios at the Arctic sites in winter and early spring. Measurement uncertainties may explain part of the discrepancy, but there is likely more room for improvement in the BC emission inventory. The long-term surface measurements cover different time periods for some sites, over which BC sources have likely changed. The simulations discussed in Wang et al. (2012a) used the IPCC AR5 emissions for the year 2000. As a result of socio-economic changes, the AR5 BC and sulfate emissions in the 1980s are quite different than those in 2000. Although the global annual emissions were lower in 1980 (6.9 Tg C yr-1) than in 2000 (7.8 Tg C yr-1), winter (DJF months) emissions integrated between 40°N and 70°N were significantly higher in 1980 than in 2000 (1.87 vs. 1.25 Tg C yr-1), with important Arctic impacts. AR5 SO_2 emissions for the years 1980 and 2000 have similar signatures for the same season and region (113% higher emission in 1980). Our sensitivity experiment with 1980 emissions shows that during DJF, the 50% higher BC emissions (compared to the year 2000 emissions) over 40°-70°N translates to a 50% higher BC burden and 70% higher BC surface mixing ratio north of 50°N. There were similar consequences to Arctic sulfate mixing ratios, highlighting the important role of emissions, particularly aerosol sources in mid/high latitudes in affecting Arctic aerosol abundance.

Regional aerosol source tagging provides quantitative aerosol source-receptor relationships and identifies transport pathways (Wang et al. 2012c). Figure 3.2 shows an example of the relative

contribution of regional sources (e.g., Europe and Asia) to monthly mean Arctic BC depends quite strongly on emissions (year 1980s vs. 2000s). This tool is being used to characterize the sensitivity of aerosol burden in receptor regions (including, but not limited to, the Arctic) to perturbations of emissions in a particular source region.

3.1.3 Impact of Aerosols on Monsoons Near Source Regions

A lot of high-latitude aerosols originate in lower latitudes, where aerosol sources and sinks are orders of magnitude higher than high latitudes. Aerosol-cloud interactions near source regions and along the pathways to the Arctic are important for the long-range transport, and changes to large-scale circulation features also influence high-latitude climate. Therefore, in FY2012, we have broadened our studies of aerosols and climate to focus more on lower latitude phenomena. We chose to start with South Asia, a region with very high concentrations of anthropogenic and natural aerosols, and also a region where aerosol sources are expected to change rapidly. These sources are likely to influence high latitudes in multiple ways. They also have impacts locally. As a result, we started by exploring some local effects, with possible changes in monsoon precipitation and circulation in response to changes in anthropogenic and natural aerosols. We completed four studies documenting various aerosol impacts on monsoons and monsoon circulations in India and Africa.

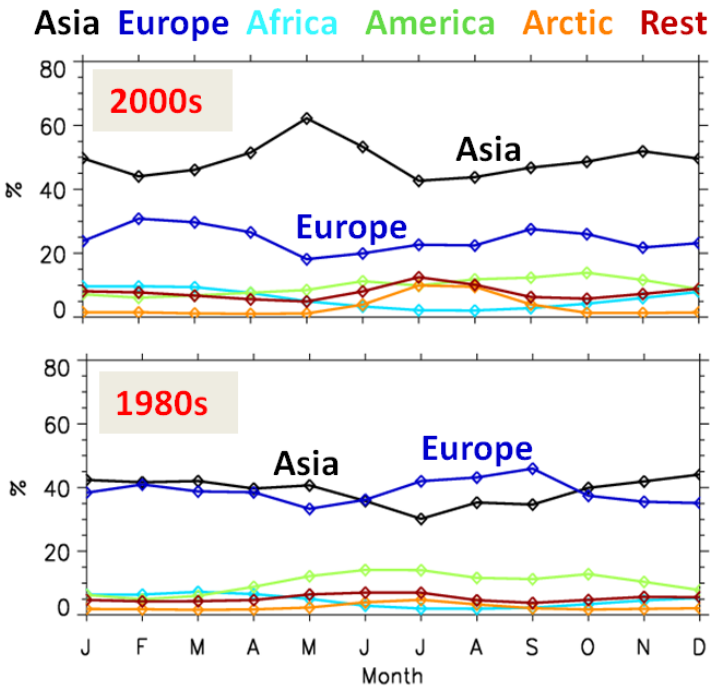

Figure 3.2. Relative contribution to monthly mean Arctic BC from various regions derived from CAM5 simulations with 1980s (bottom) and 2000s (top) emission inventories, respectively. (Wang et al. 2012c).

Ganguly et al. (2012a) showed anthropogenic and biomass burning aerosols generally reduce summer monsoon precipitation over most areas of the Indian subcontinent, but modest increases also occur over the northwestern part of the subcontinent. Much of the reduction in precipitation is triggered by local aerosol emissions from anthropogenic activities, but modest precipitation increases in the northwest were associated with decreases in local emissions of aerosols from forest fire and grass fire sources.

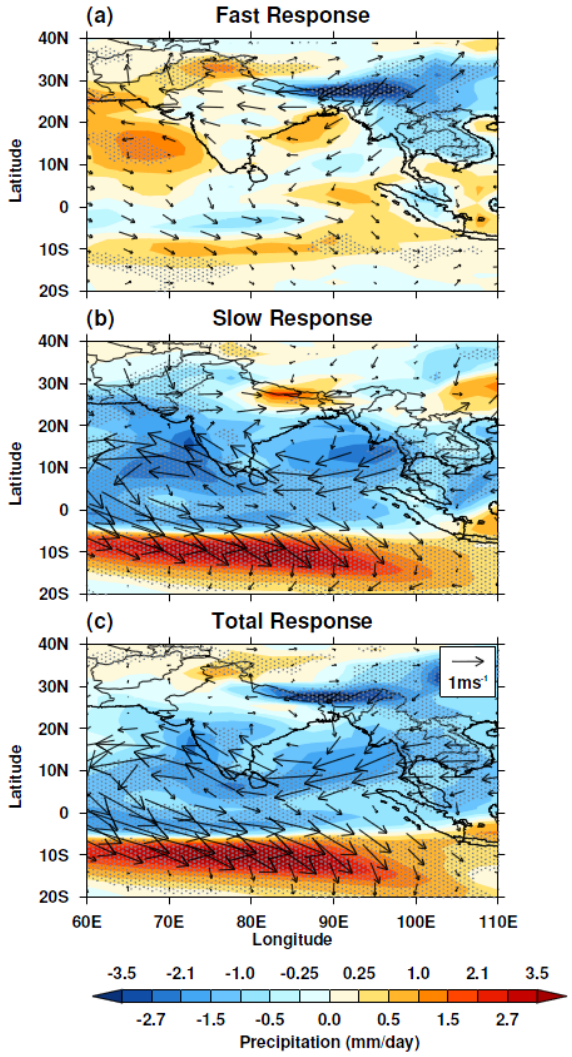

Figure 3.3. JJAS mean (a) fast, (b) slow, and (c) total responses in precipitation and wind vectors at 860 hPa to present day aerosol forcing. Stipples in all panels represent areas where the anomalies (in precipitation) are at or exceed the 90% confidence level based on the student's t-test. (From Ganguly et al. 2012b).

Anthropogenic aerosols from outside Asia also contribute to the overall reduction in precipitation, but the dominant contribution comes from local sources. Local emissions play a more important role in rainfall from anthropogenic aerosol sources during the early monsoon period; local and remote emissions of aerosols become equally important during the latter part of the monsoon period. By as much as a factor of two (preserving their ratio), changes in local anthropogenic organic and black carbon emissions produce the same basic signatures in the model's summer monsoon temperature and precipitation responses. While precipitation responses are primarily driven by local aerosol forcing, regional surface temperature changes over the region are strongly influenced by anthropogenic aerosols from remote sources.

Ganguly et al. (2012b) explored the fast and slow responses of the South Asian monsoon system to anthropogenic aerosol forcing. The authors found that the feedbacks associated with sea surface temperature (SST) change caused by aerosol forcing plays a more important role than the aerosol's direct radiative impact on radiation, clouds, and land surface (rapid adjustments) in shaping the total equilibrium climate response of the monsoon system to aerosol forcing (see Figure 3.3).

Vinoj et al. (2012) used both observational evidence and numerical modeling results to demonstrate a remote aerosol link to the Indian summer monsoon rainfall, which is (over central India) positively correlated with aerosols over Arabian Sea and West Asia. CAM5 simulations support this remote aerosol link and further demonstrate that dust particles over West Asia through fast responses (e.g., solar heating and cloud thermodynamics) induce additional moisture transport and convergence over central India, resulting in increased monsoon rainfall. However, sea salt aerosols tend to have an opposite effect and reduce rainfall. This finding highlights the importance of natural aerosols in modulating the strength of the Indian summer monsoon, suggesting research on the long-term trends in monsoon precipitation needs to consider changes in background aerosols of natural origin as well.

Subtropical North Africa has been subject to extensive droughts in the late 20th century, which are frequently linked to changes in the SST in both the Atlantic and Indian Oceans. However, climate models

forced by observed SSTs were unable to reproduce the magnitude of observed rainfall reduction over the last several decades. In an African monsoon study (Yoon et al. 2012b), we propose that aerosol indirect effects (AIE) may be an important positive feedback mechanism to contribute this recent reduction. Two sets of CAM5 sensitivity experiments were designed to distinguish the role of aerosol direct/semi-direct and indirect effects on regional precipitation. Changes in cloud lifetime due to the presence of carbonaceous aerosols are found to be a key mechanism to explain the reduced rainfall over subtropical North Africa. We have also analyzed coupled simulations to study the impact of anthropogenic aerosols on the Sahel drought in the 1970s and recovery in 1990s, which is discussed in a later section.

3.1.4 Prescribed-aerosol Capability of CAM5

Aerosol process calculations are computationally expensive. For some applications, it is desirable to prescribe rather than predict aerosol mass and number concentrations in global climate models such as CAM5/CESM1. The objectives of this project task were to: (1) develop a new capability for CAM5 to use monthly archived aerosol properties, and (2) produce a climate with the prescribed-aerosol capability that should be virtually identical to simulations with predicted aerosols, reducing computational cost, and allowing various aerosol processes to be easily isolated. For example, to isolate process interactions, one can provide "prescribed values" to some model processes but predicted values for others.

In the past year, a couple of strategies were developed and tested. Conditionally sampled aerosol quantities were first used, rather than monthly mean values, in order to account for aerosol removal processes when clouds are present. These simulations often produced a similar climate to the control simulations with predicted aerosol distributions, except for the excessive Arctic low clouds during northern summer season (see Figure 3.4 (b) and (c)). These discrepancies are associated with exceptionally low aerosol values over the Arctic in summer (Figure 3.4 (a)). To solve this problem, we developed a new approach based on "stochastic sampling from a log-normal distribution". Instead of prescribing monthly mean values, we prescribe the PDF of the aerosol quantity and randomly sample values from the PDF. With this method, the CAM5 model quite closely reproduces the model climate with predicted aerosols. We are preparing code for release in the CAM5 model and preparing a manuscript describing the method and scientific applications (Yoon et al. 2012c).

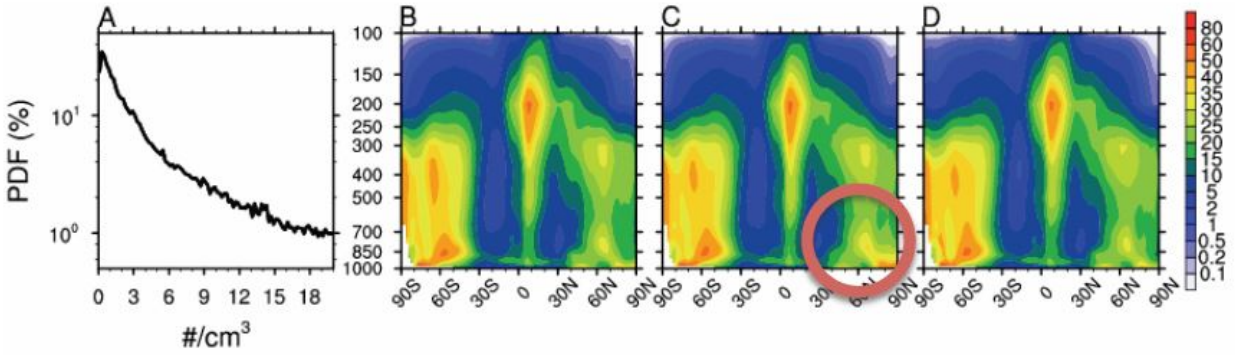

Figure 3.4. (a) PDF of accumulation mode aerosol number concentration for CAM5.1 for all gridpoints poleward of 80N. (b) Zonal mean cloud fraction for fully standard interactive aerosol, (c) for prescribed monthly mean aerosol, and (d) for a stochastic parameterization of aerosol number. The circled red region indicates the region where the simpler prescribed-aerosol parameterization fails.

3.1.5 Aerosol Speciation

Although CAM5 simulates all of the major aerosol species (sulfate, organic carbon, black carbon, mineral dust, and sea salt) for multiple internally mixed modes, it neglects the diversity of composition and properties of organic carbon and mineral dust. To account for this diversity, we modified the code to distinguish between black carbon (BC) and primary organic matter (POM) through fossil fuel and biomass burning combustion for both MAM3 and MAM7, and worked with collaborators (Natalie Mahowald and her student Rachel Scanza) to speciate mineral dust into five internally mixed mineral species (Claquin et al. 1999; Hoose et al. 2008). Speciating BC allows CAM5 to distinguish between direct radiative forcing by fossil fuel and biomass burning combustion. Speciating POM allows CAM5 to use different hygroscopicity κ and refractive index for POM from fossil fuel and biomass burning, which affects removal of BC emitted with POM. Speciating mineral dust permits use of different κ, ice-nucleating ability, and refractive index for the different species of mineral dust. These code modifications are being merged onto a single developmental branch of CAM5 for further development and experiments by our collaborators in the CESM community. Dr. Nicholas Meskhidze will apply his marine organic code (Meskhidze et al. 2011; Gantt et al. 2012) to this branch. We have already used the BC and POM speciation in simulations used in the AeroCom (Myhre et al. 2012) and Atmospheric Chemistry and Climate Model Intercomparison Project (ACCMIP) (Shindell et al. 2012; Lee et al. 2012) model intercomparison activities to determine the impact of using more realistic physical properties for POM.

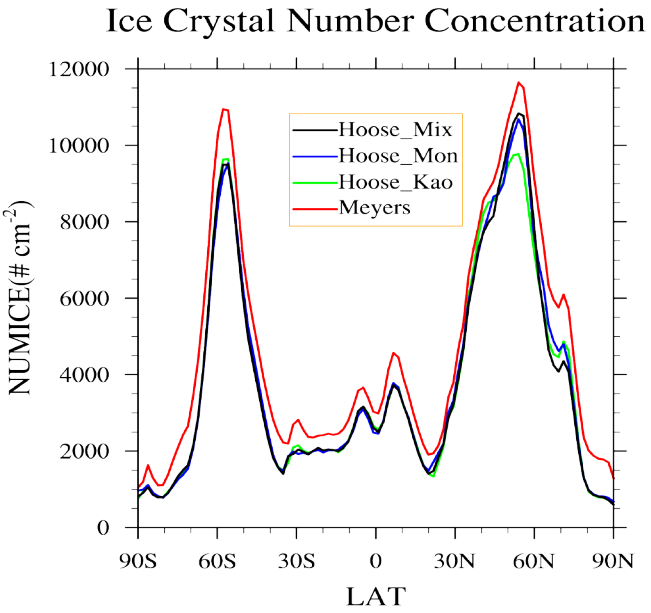

Figure 3.5. Zonal and annual mean column integrated ice crystal number concentration in mixed-phase clouds simulated by CAM5 with the Meyers et al. (1992) treatment of ice nucleation (Meyers), with the Lohmann and Diehl (2006) treatment of immersion nucleation for montmorillonite applied to all dust (Hoose_Mon), with the Lohmann and Diehl (2006) treatment for Kaolinite applied to all dust (Hoose_Kao), and with the Lohmann and Diehl (2006) treatments applied to each dust specie (Hoose_Mix).

In CAM5, the κ and refractive index of POM from biomass burning are assumed to be the same as for POM from fossil fuel combustion. Measurements indicate that the POM from biomass burning is significantly more hygroscopic than POM from fossil fuel combustion (Liu and Wang 2010), but such a distinction is not possible in CAM5 because only one POM specie is simulated by CAM5. With the introduction of speciation, we can now use different κ values for POM. These different values will influence water uptake on particles composed of POM, droplet formation on particles with POM, and the rate of nucleation scavenging of the POM. As POM and BC are co-emitted, a sensitivity simulation that uses a more realistic κ value for both POM from fossil fuel combustion (0.0) and POM from biomass burning (0.2)

also shows the impact on the burden of POM and BC burdens. The larger POM κ increases water uptake on particles containing POM as well as absorption efficiency of particles composed of internal mixtures of POM and BC. We are writing a paper to document detailed analyses and evaluation.

While our collaborators are focusing on the impact of dust speciation on dust optical properties and radiative forcing, we have applied the dust speciation to ice nucleation by immersion freezing and contact nucleation, following Hoose et al. (2008) and Lohmann and Diehl (2006). Figure 3.5 shows that the column ice crystal number concentration is about 10% smaller with the Lohmann and Diehl (2006) treatments compared with the Meyers et al. (1992) ice nucleation scheme in CAM5. Because of negative feedbacks between cloud liquid water content and immersion nucleation rate, there is much less sensitivity of column ice crystal number concentration to dust speciation.

3.1.6 New Aerosol Module MAM4

BC aging during long-range transport may strongly affect Arctic BC. CAM5 employs a modal aerosol module (MAM) to represent the log-normal size distributions of aerosols (Liu et al. 2012). Two variants are available, a faster three-mode (MAM3) "production" variant or a seven-mode (MAM7) "benchmark" variant. The major difference between MAM3 and MAM7 related to BC lies in treatments of the primary carbon mode and accumulation mode. In MAM3, BC is assumed to be instantaneously internally mixed and it shares the same hygroscopicity with organic carbon (POM) in the accumulation mode. Depending on the concentration of sulfuric acid gas and the availability of other soluble species in the same mode, BC-containing particles can be transformed into a soluble state within one model time step, producing a very fast BC aging. However, in the MAM7, hydrophobic BC and OC are emitted into the primary carbon mode in which particles take time to grow/age into the accumulation mode through condensation of gas-phase species and coagulation with soluble particles in other modes. Therefore, BC aging may be strongly influenced by these processes, for example, by varying the number of monolayers of sulfate coating for converting a fresh BC/POM particle to the accumulation mode. The additional primary carbon mode itself does not improve the Arctic BC simulation significantly with the MAM3 aerosol module, but slower BC aging in MAM7 can substantially increase Arctic BC (Liu et al. 2012; Wang et al. 2012a).

However, the MAM7 is not optimal for longer-term climate simulations because it is very computationally expensive (e.g., it doubles the number of aerosol tracers in MAM3). To improve the prediction of BC in CAM5 and to be computationally manageable, we have developed a new version of MAM with four aerosol modes (MAM4), which is MAM3 plus the primary carbon mode for POM/BC like that in MAM7, with consideration of the explicit aging process of primary POM/BC particles. It introduces three additional aerosol tracers on top of the existing 15 for MAM3. The MAM4 has been implemented in CAM5 as an additional configuration option (trop_mam4). We performed sensitivity simulations and evaluated them against observations. MAM4 is shown to significantly improve the BC simulation in the Arctic as the MAM7 does (see Figure 3.6 for an example) but with ~10% increase in the total CAM5 computational time. We plan to complete the evaluation and use it in our coupled climate simulations in FY2013.

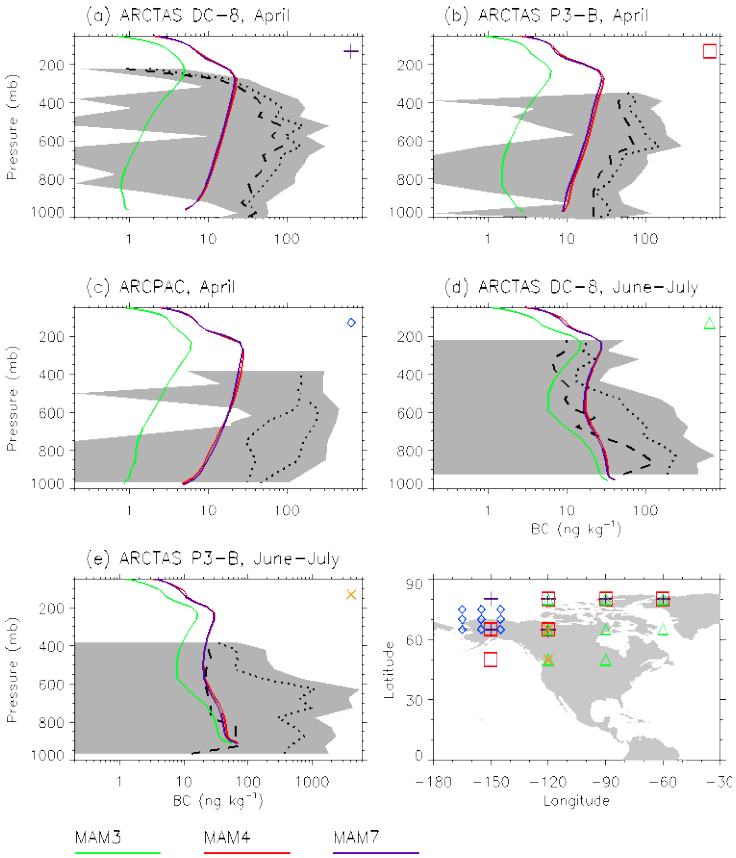

Figure 3.6. Observed and simulated BC vertical profiles at high latitudes from two campaigns: NASA Arctic Research of the Composition of the Troposphere from Aircraft and Satellite (ARCTAS), and NOAA Aerosol, Radiation, and Cloud Processes affecting Arctic Climate (ARCPAC). See Koch et al. (2009) for details on the campaign data.

3.2 Clouds

Clouds strongly influence the radiative budget of the Arctic and the planet, and as indicated above, play an important role in influencing aerosols reaching the Arctic. The emphasis over the past year has been on stratiform clouds.

3.2.1 Stratiform Cloud Physics

Clouds arise from complicated interactions between many physical processes, most of which must be parameterized in global models. However, coupling between parameterizations is often crude, and assumptions used for one process are often inconsistent with those used for others. Poor interaction between processes is thought to be a major source of deficiencies in CAM5.

Previous years' efforts for this project centered on developing Gaussian PDF-based liquid macrophysics (condensation/evaporation + cloud fraction) and microphysics (deposition, freezing, and precipitation) schemes for CAM5, as well as identifying and correcting issues associated with the coupling between macrophysics and microphysics. This year, efforts have centered on evaluating and improving these changes.

Our model changes were found to greatly improve model LWP and shortwave cloud forcing. Other aspects of model behavior are no worse than the default model. Aerosol sensitivity is slightly increased due to an increase in shortwave indirect effect that is not quite compensated by increased longwave indirect effect. Because CAM5 aerosol sensitivity is already thought to be too high, we are trying to understand and potentially reduce this sensitivity. Climate sensitivity appears to be approximately unchanged (after model improvements, climate sensitivity decreases from 4.1 to 3.9 K for CO_2 doubling). We are currently writing a paper documenting our changes and their impacts (Caldwell et al. 2012a).

One discovery this year is that using an unbounded PDF for liquid macrophysics has a substantial and detrimental effect on ice cloud fraction in polar regions. A partial explanation for this is a step-wise enhancement of the vapor deposition rate in the presence of vanishing small cloud liquid. Deposited vapor is then removed by sedimentation, resulting in significantly decreased relative humidity and decreased ice cloud fraction in cold, dry regions. We are still trying to understand the remaining source of sensitivity. This issue is important because many other groups use unbounded PDFs for macrophysics, and our results likely transfer to their work as well.

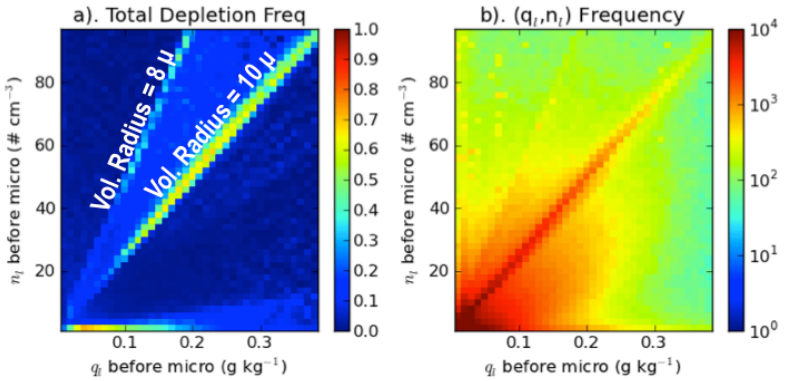

Figure 3.7. The first panel shows the frequency of microphysics starting with enough liquid to operate and depleting it all within a timestep (colors) as a function of liquid water content and droplet concentration. The second panel shows the frequency of encountering given liquid water content and droplet concentration conditions. Both panels are based on a month of ½ hourly global data at ~750 mb.

Another mystery solved this year is why CAM5 microphysics runs out of liquid water every timestep over most of the globe. This is a problem because, as noted by other work funded by this project (Sednev and Menon, 2012), numerical timestepping becomes ill-posed when the depletion timescale of a process becomes shorter than the model timestep. These total depletion cases occur where liquid is detrained from convection. Detrained liquid is assumed to have an 8 or 10 μm volume mean radius (for deep and shallow convection, respectively), which shows up as bands in Figure 3.7. Depletion occurs because the temperature and drop-size assumptions used for detrainment are inconsistent with those used in microphysics. In particular, liquid/ice partitioning of detrained condensate uses a simple temperature weighting, which microphysics tries to correct by rapidly freezing detrained water. Because of process ordering within microphysics, this occurs via vapor deposition rather than droplet freezing, which means that detrainment adds mass but not particle number. Much of the detrained condensate is also immediately converted to rain. This occurs because, in contrast to the detrainment code, microphysics assumes droplet size follows a gamma PDF, implying that many larger drops tend to rain out. We are currently writing a paper describing this case in detail (Caldwell et al. 2012b). This study suggests the need to rethink the

coupling between convection and processes within microphysics. Hopefully, this will be accomplished mainly through others' efforts to include microphysics within the convective schemes, but Dr. Peter Caldwell will probably be tangentially involved as an advisor to the CAM microphysics developers.

3.3 Aerosol and Cloud Assessment

Validation of models requires an assessment of model results compared to observational data and/or high-resolution model simulations. We are assessing the role of cloud and aerosol processes by comparing them with a variety of data, from ARM to satellite data, and using a variety of methods and tools.

3.3.1 Evaluation of CAM5 Physics and Model Resolution Using Regional WRF

Improving process representation in CAM5/CESM is the primary focus of this project. However, we use the regional Weather Research and Forecasting (WRF) model as a testbed for assessing existing physics parameterizations and those being implemented into CESM. The WRF model can be run at a much finer spatial resolution than the CESM. Hence, it can be used to bridge the gap between site measurements and CESM grids and to quantify errors in CESM due to unresolved mesoscale processes and surface conditions that affect clouds and aerosol-cloud interactions. This WRF configuration also allows us to investigate CAM5 parameterizations at very high resolutions, providing insight into CAM behavior at high resolution. We have successfully coupled large-scale CAM5 simulations with mesoscale WRF simulations to investigate the effects of the resolution on cloud and aerosol properties in the Arctic and other regions globally (see Figure 3.8 for an illustration). We are currently working on a paper (Ma et al. 2012b) to describe the downscaling of CAM5 physics parameterization to WRF.

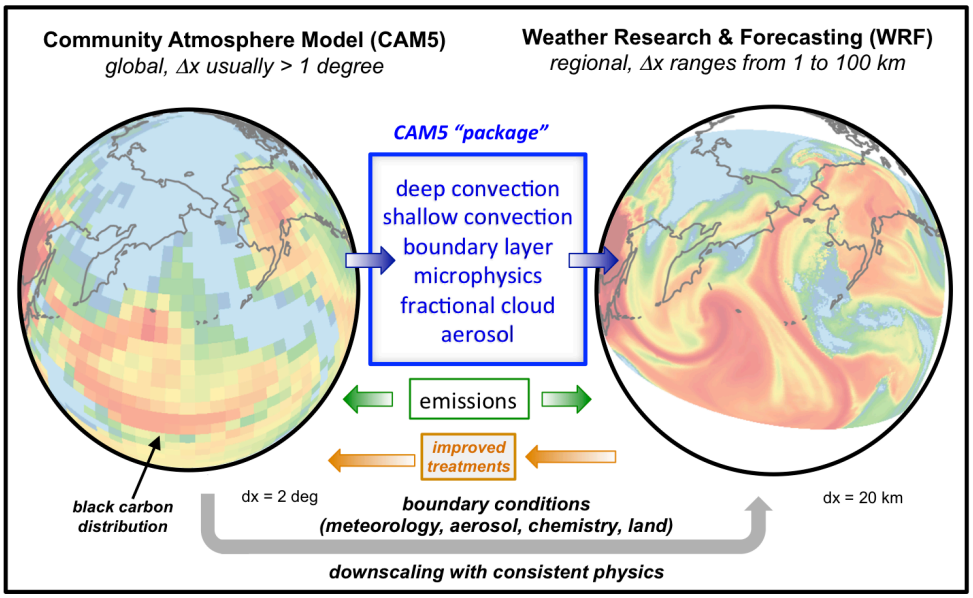

Figure 3.8. Schematic diagram depicting the coupling of CAM5 physics parameterizations to the regional WRF model. The background color plots are BC distributions simulated by CAM5 (2 degree) and WRF (20 km) with the same physics parameterizations. (From Ma et al. 2012b).

In a separate study (Ma et al. 2012c), we explore the resolution dependence of CAM5 physics by comparing WRF-Chem simulations (with CAM5 physics) run at various horizontal grid-spacings (10, 20, 40, 80, and 160 km). The results are evaluated against the Indirect and Semi-direct Aerosol Campaign (ISDAC) field campaign data. We find that CAM5 physics produces higher cloud LWPs and higher aerosol concentrations with increasing resolution. We also find that mesoscale eddies are better resolved in high-resolution simulations, producing filaments of concentrated aerosol plumes that are responsible for higher aerosol loading episodes observed over Barrow, Alaska associated with "Arctic haze". The

aerosol plumes and the clouds are less often collocated in the high-resolution runs, resulting in less wet scavenging. Simulations also show (Figure 3.9) a decreasing trend of susceptibility of cloud LWP to aerosol loading as resolution increases.

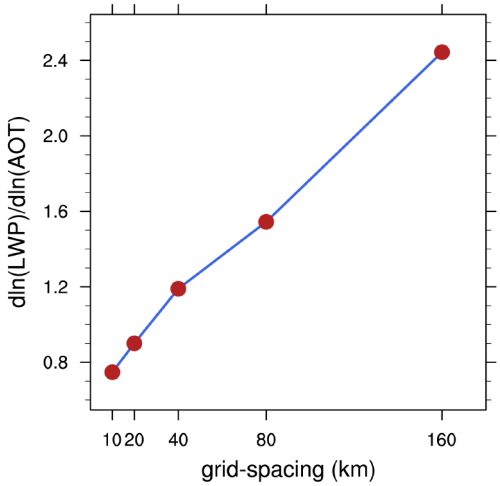

Figure 3.9. The relative change of liquid water path (LWP) to aerosol optical thickness (AOT) as a function of model grid spacing in WRF (with CAM5 physics).

We have begun simulations to track biomass burning plumes from their sources to the Arctic and assess the impact of resolution on the resulting chemistry, transport, and mixing that affects the resulting concentration of BC and other aerosol species reaching Alaska.

3.3.2 Assessment of Arctic Lower Tropospheric Stability

CMIP3 models generally have a more stable Arctic lower tropospheric stability than reanalysis or observations indicate (Mederios et al. 2011). In addition, it has been theorized that an overly stable Arctic lower troposphere leads to an unrealistic negative feedback to climate change (Boe et al. 2009). In order to provide insight into why GCMs have this bias, we examine the lower tropospheric stability bias in CAM4 and CAM5. CAM4 and CAM5 are run in forecast (e.g., CAPT) and AMIP mode. Indeed, both CAM4 and CAM5 show drifts to overly stable states within the first few days of hindcasts at a level that reaches an appreciable fraction of the bias exhibited in AMIP integrations (Figure 3.10). These drifts are larger during winter months, and are mainly a result from a near surface cold bias.

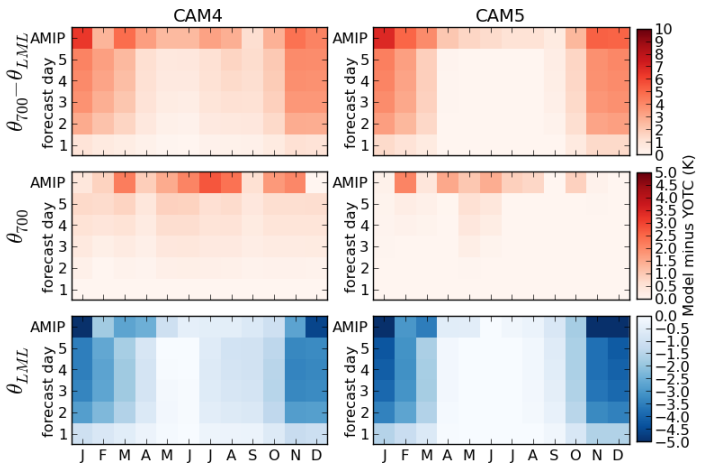

Figure 3.10. Biases in lower-tropospheric stability (top), potential temperature at 700 hPa (middle), and potential temperature (bottom) at the lowest model level (LML) for CAM4 (left) and CAM5 (right). The biases are averaged poleward of 60°N and are measured with respect to ECMWF analysis. The x-axis indicates month and the y-axis indicates the hindcast day in which models were analyzed with the top row illustrating bias in AMIP mode.

This bias is analyzed across the Arctic domain (seen in Figure 3.10), and locally at the ARM NSA site where *in situ* data aid in determining reasons for the bias. Analysis at the ARM NSA site confirms that the lower tropospheric stability bias occurred when the surface is becoming colder than observations. In addition, the lower tropospheric stability bias arose when opaquely cloudy periods occurred in the observations, but the radiative clear periods occurred in the models. The models have too many periods of radiative clear skies compared to the observations. This results in a deficient of downwelling longwave radiation and a colder surface. The analysis at the ARM NSA site is consistent with the comparison between CALIPSO and the models' CALIPSO simulators across the Arctic domain (Barton et al. 2012). A paper describing this work is currently in preparation (Barton et al. 2013).

3.3.3 Assessment of Cloud Response to Arctic Surface Type using CALIPSO

The cloud response to changes in Arctic surface type is an interest in a warming Arctic with less sea ice. The cloud response to sea ice was examined by controlling for dynamics and thermodynamics, which is different than previous studies that only examined clouds when sea ice was or was not present (e.g., Schweiger et al. 2008; Kay and Gettelman 2009; Palm et al. 2010). To control for dynamics and thermodynamics, a k-means cluster algorithm was used to determine dominant Arctic synoptic regimes. Lower tropospheric stability and mid-tropospheric vertical velocity were used as inputs to the algorithm.

Three regimes were found that had mid-tropospheric subsidence, and these regimes were separated by differences in lower tropospheric stability. These regimes were called high stability, very-high stability, and stable. One regime was associated with mid-tropospheric uplift. CALIPSO cloud fractions that occurred during these regimes were composited and then separated by surface type (i.e., sea ice, open ocean, and land). In going from sea ice to open ocean, the CALIPSO cloud fraction increased at the lowest atmospheric levels for all subsidence regimes, except the stable regime. In addition, the cloud height increased for all subsidence regimes except the very-high stability regime. There was not a large response of clouds to surface type for the uplift regime (Figure 3.11).

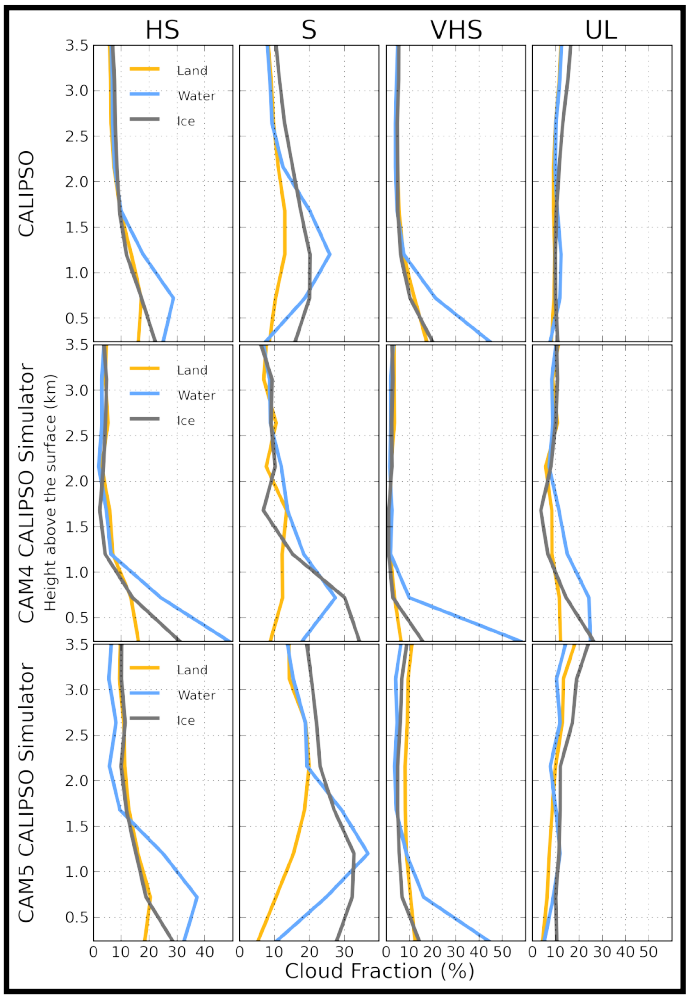

Figure 3.11. The (top) CALIPSO, (middle) CAM4 CALIPSO simulator, and (bottom) CAM5 CALIPSO simulator cloud percentages for each synoptic regime separated for periods that occurred over (blue line) water, (orange line) land, and (grey line) sea ice locations. Sea ice periods were defined as locations in which the grid box sea ice concentration was greater than 15% for each temporal step. The synoptic regimes from left to right are the High Stability (HS), Stable (S), Very-High Stability (VHS), and UpLift (UL).

How well do CAM4 and CAM5 reproduce this observed variability? CAM4 and CAM5 were run in forecast mode for the same analysis time period previously described. In addition, the cloud fractions from the CAM4 and CAM5 CALIPSO simulator were composited using the method previously described. CAM5's cloud response to surface type was more similar to observations than CAM4's response (Figure 3.11). In going from a sea ice covered surface to open water, the CAM4 CALIPSO simulator cloud fractions at the lowest atmospheric levels increased for all regimes, which was not consistent with observations. A paper fully describing these results has been published (Barton et al. 2012).Assessment Using ARM Data

Aerosol first indirect effects on non-precipitating low liquid cloud properties simulated in CAM5 for YOTC Period

Indirect effects of aerosols are considered to be one of the most uncertain components in forcing of climate change over the industrial period. Since various aerosol-cloud interactions are often associated with the change of cloud droplet size distribution by aerosol pollution, we first study the aerosols' first indirect effect (FIE) at three Department of Energy (DOE) Atmospheric Radiation Measurement (ARM) sites based on a series of five-day CAM5 forecast runs by the DOE-supported Cloud-Associated

Parameterizations Testbed (CAPT) project for the period of Year of Tropical Cyclone (YOTC) from June 2008 to May 2010. To better compare with the conditions observed in previous studies, we examined non-precipitating low-level, single-layer, overcast warm (liquid-phase only) clouds. We examined the relationship of cloud droplet effective radius (re) to both the number concentration of aerosols in the accumulation mode and the number concentration of cloud condensation nuclei at 0.1% supersaturation.

Our study (Zhao et al. 2012) shows that the FIE values obtained from CAM5 hindcast simulations usually lie within the range calculated from a large number of observation studies. This suggests that the new double-moment cloud microphysics and interactive aerosol model parameterizations work reasonably well, at least for this cloud type and at the ARM sites. Theses results also suggest that if CAM5 and other global climate models overestimate the magnitude of indirect effects, as is widely perceived, then the problem may lie in the representation of the second and other indirect effects and not with the representation of the FIE. The study also shows that aerosol FIE is sensitive to the cloud LWC, cloud location, time, and aerosol variable that represents its amount. In general, the aerosol FIE decreases with LWC and is slightly larger over ocean than over land due to the pollution differences. We also found that sufficient cloud samples and a narrow LWC range are essential to reasonably quantify the aerosol FIE along with the clear classification of examined cloud types.

In the future, we will separate the impacts of aerosol-cloud interactions from large-scale dynamic effects based on CAM5 forecast runs. We will then examine the variability of aerosol-cloud interactions and the climate responses to different representation of aerosol-cloud interactions, with the support of long-term ARM ground observations and satellite observations of aerosol and cloud properties.

3.3.4 CFMIP Observation Simulator Package

COSP converts model clouds into pseudo-satellite observations with a model-to-satellite approach that mimics the satellite view of an atmospheric column with model specified physical properties. The approach makes consistent assumptions and accounts for observational limitations of the satellites, including instrument signal-to-noise ratios and signal attenuation. Currently, COSP enables the comparison of model outputs with observations from six satellite platforms, including passive and active sensors. COSP is now used worldwide by most of the major models for climate and weather prediction, and it will play an important role in the evaluation of models that will be reviewed by the next report of the IPCC. COSP facilitates a more rapid improvement of climate models and will ultimately reduce uncertainty in climate predictions.

Steve Klein and Yuying Zhang joined the COSP development with scientists worldwide. In this review period, after the successful development and implementation of the COSP, we focus on the application of COSP to climate model evaluation. The representation of clouds by climate models is a key ongoing challenge, and large efforts have been undertaken with the ultimate goal of improving modeled clouds. We examined the simulated clouds in the CMIP3 and CMIP5 models using the ISCCP simulator to see if cloud simulations are improving in latest climate models. This high profile work has been summarized in a strong *Journal of Geophysical Research* paper (Klein et al. 2012). This work indicates that newer climate models have improved simulations of cloud optical depth and have fewer compensating errors in their radiation budget.

After we integrated COSP into CAM4/CAM5 with NCAR collaborators in the previous review period, the COSP-enabled CAM4/CAM5 code as a part of the CESM-1.0.3 has been released to the

climate modeling community. In order to quantify climate-modeling uncertainty, our local uncertainty quantification (UQ) team runs the perturbed-parameter ensembles with the inline COSP. Clouds vary significantly over a range of climate regimes controlled by different dynamics and physics, and problems at the regional scale can be masked by compensating errors in global or large-scale analysis. We used the ISCCP simulator output from the 337 ensemble simulations, sampling the uncertainties of 28 model parameters describing subgrid-scale processes, to systematically examine region dependencies of the CAM4 on uncertain physical parameters. Our goal is to understand which parameters and associated physical processes are most important to improving climate model-simulated clouds.

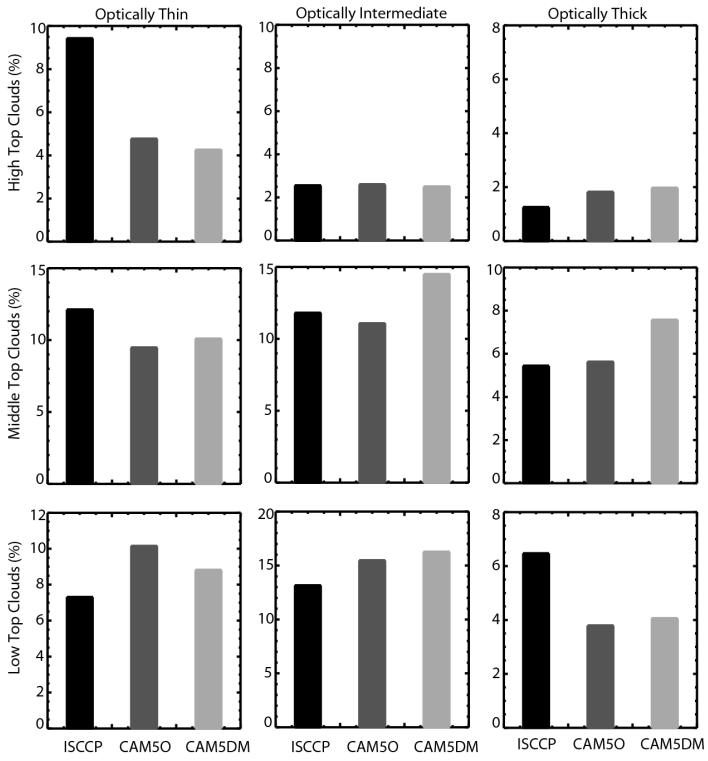

Figure 3.12. The cloud frequency for the nine ISCCP cloud types in ISCCP and the ISCCP simulator in CAM5O and CAM5DM averaged between March and September over the Arctic region (600N–800N). The high-, middle-, and low-top clouds are defined as those with cloud top pressure less than 440 hPa, between 680 hPa and 440 hPa, and larger than 680 hPa, respectively. The optically thin, intermediate, and thick clouds are defined as those with the cloud optical depth in the range of 0.02-3.6, 3.6-23, and larger than 23, respectively. The comparison with satellite data indicates the new scheme has slightly improved optically thin low cloud simulations, but produced too many optically thick middle and high clouds.

Results show the model performance is quite sensitive to parameter values over different cloud regimes. Some parameter setups could yield overall better simulations than the default CAM4 for different cloud types in different climate regimes. These include decreased relative humidity threshold for low stable clouds and precipitation efficiency for deep convection. In contrast, the improvement of other parameter values may be regional dependent for some types of clouds. These results indicate the cloud simulation might be improved by carefully adjusting some parameters, and at the same time present some

challenges for other parameters. More importantly, understanding why certain setups give overall better performance than the default configuration may benefit more climate model development processes. This study has been published in *Geophysical Research Letters* (Zhang et al. 2012).

3.3.5 Sensitivity of CAM5 Simulated Arctic Clouds and Radiation to Ice Nucleation Parameterization with Satellite and ARM Data

To better understand the important role of ice nucleation processes in clouds and radiation simulated by climate models, we tested a new ice nucleation parameterization developed by DeMott et al. (2010) in CAM5, to replace the Meyers et al. (1992) parameterization. The new scheme is a more physically based ice nucleation scheme that links the variation of ice nuclei (IN) number concentration to aerosol properties (i.e., aerosol particles with diameter larger than 0.5 μm), while the CAM5 default scheme parameterizes the IN number concentration simply as a function of ice supersaturation. Specifically, we focused on how modeled cloud types and their properties vary with the treatment of ice nucleation processes and what impact these changes have on the Earth's radiation budget.

The new scheme has led to a significant reduction in simulated IN number concentrations in the Arctic region. This has resulted in a noticeable increase in mid- and high-level clouds and a decrease in low-level clouds. The smaller IN concentrations result in a considerable increase of cloud LWP and decrease of ice water path. Overall, there is an increase in cloud optical depth of Arctic clouds, which leads to a stronger shortwave, longwave, and net cloud radiative forcing (cooling) at the top of the atmosphere. The comparison with satellite data by using the CAM5 COSP simulator indicates that the new scheme has slightly improved the fidelity of optically thin low clouds, but produced too many optically thick middle and high clouds (Figure 3.12). A further comparison with ARM Arctic long-term ground-based measurements at its Barrow site shows that the new scheme has led to a clearly better simulation of clouds and their properties, which helps reduce model errors in surface radiation (Figure 3.13). In turn ,the changes in cloud properties impact aerosol simulations in the Arctic, which is to be examined in a future study.

Results from this study indicate the importance of better representation of the ice nucleation process in mixed-phase clouds in climate models in the Arctic region. Linking ice nucleation parameterization to aerosol properties allows climate models to better represent aerosol-cloud coupling. However, this requires more accurate simulations of aerosol fields in climate models. Like most climate models, CAM5 has the low bias in aerosol concentration in the Arctic transported from midlatitudes (Liu et al. 2012), due to very efficient wet removal of aerosols. Recent studies (e.g., Wang et al. 2012) have shown that improved representations of aerosol (e.g., for aerosol aging and transport and removal of aerosols in convective clouds) and cloud microphysics and macrophysics have significantly improved the aerosol simulations, especially in high latitudes. More robust evaluations of physically based ice nucleation schemes could be done with improved aerosol simulations and observations in the future. A manuscript that summarizes the current study was submitted to *Journal of Climate* and is currently under revision (Xie et al. 2012).

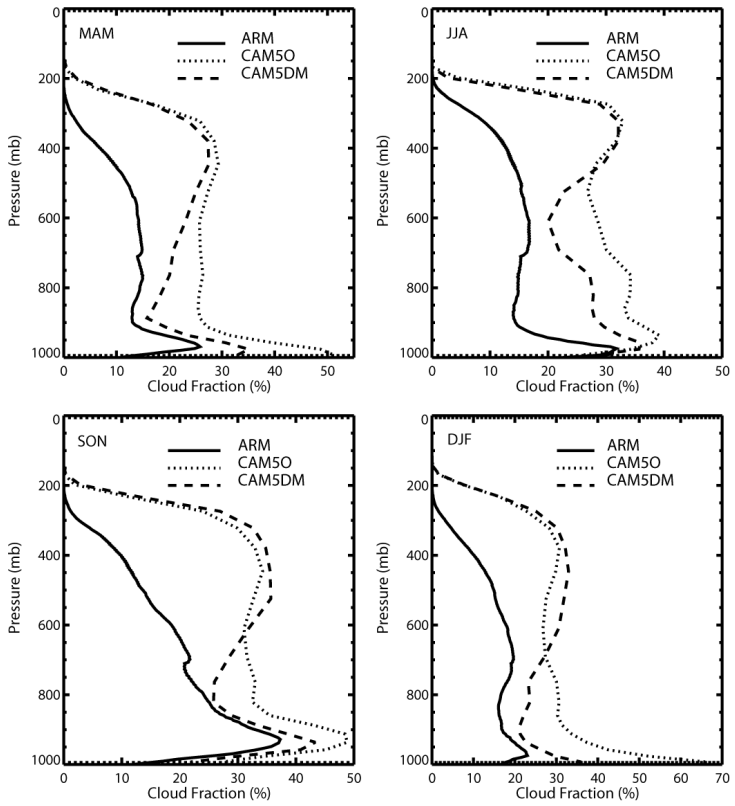

Figure 3.13. Vertical profiles of the seasonal mean cloud fraction from the two CAM5 six-year simulations (the control run CAM5O and the run with the DeMott et al. (2010) ice nucleation parameterization, CAM5DM) with ARM observations. Both models largely overestimate the observed cloud fraction for all the seasons. CAM5 considerably improves the model simulations with the DeMott et al. ice nucleation parameterization.

3.3.6 Tools to Calibrate Model and Assess Aerosol Indirect Effects

Parameterization sensitivity to uncertain parameters and optimization

Tunable parameters are often used in climate model parameterizations. Determination of values for these parameters is typically based on theoretical calculations or limited measurements. Adjustments of parameter values are often needed to better match model simulations with observations. However, improvements in model skill score associated with the given parameter values may have compensating errors in different local or even non-local physical processes. Calibration or optimization of model parameters is important not only for reducing model uncertainties but also for better understanding of the processes within the climate system. In a recent study (Yang et al. 2012), we applied an UQ technique to improve the modeling of convective precipitation in CAM5, where convective and stratiform precipitation partitioning is very different from observational estimates. We examined the sensitivity of precipitation and circulation to key parameters in the Zhang-McFarlane deep convection scheme, using a stochastic importance-sampling algorithm that can progressively converge to the optimal parameters. The most sensitive parameters were identified, and then optimized using TRMM satellite measurements of convective precipitation. The optimized parameter set remarkably improved the CAM5 simulation of the convective-to-stratiform precipitation ratio and the rain intensity spectrum. The impact of improved deep convection on the global circulation and climate was also evaluated. Moreover, there were positive

impacts on some aspects of the atmospheric circulation and climate, such as the reduction of the double ITCZ, improved East Asian monsoon precipitation, and improved annual cycles of the cross-equatorial jets. We plan to continue using this tool to calibrate/optimize parameterizations in CAM5, when appropriate, to optimize their behavior for features that have not previously been considered in tuning/calibration.

Rain frequency susceptibility as a metric to evaluate aerosol-cloud-precipitation interactions in global climate models

We recently developed a new metric, called rain frequency (or probability of precipitation) susceptibility to aerosols (S_{pop}), to evaluate aerosol-cloud-precipitation interactions in global climate models, and to further constrain cloud lifetime effects of aerosols (M Wang et al. 2012), partially funded by this project. Here, rain frequency susceptibility is a quantitative measure of how the probability of precipitation for clouds at a given LWP is sensitive to aerosol concentrations. Results based on two conventional aerosol-climate models (CAM5 and ECHAM5), and one multi-scale aerosol-climate modelb were used to demonstrate that S_{pop} is a robust measure of the LWP response to a perturbation in CCN concentrations (λ=dlnLWP/dlnCCN). Therefore, the strong link between S_{pop} and λ provides a way to use satellite observations to constrain cloud lifetime effects of aerosols. Our results showed that S_{pop} derived from A-Train satellite observations is substantially smaller than those simulated in global climate models, and implied substantially smaller cloud lifetime effects of aerosols (a reduction by one-third of that in CAM5). Our results further showed that the large cloud lifetime effect of aerosols in CAM5 is related to the likely too strong role of autoconversion in rain formation in CAM5. In another study partly supported by this project, Rosenfeld et al. (2012) found that cloud drop effective radius (r_e) plays a predominant role in determining rain properties in marine stratocumulus, which is in agreement with recent aircraft observations and theoretical studies in convective clouds. This study provides the basis for a new autoconversion scheme that directly incorporates r_e and a simple parameterization of rain rate for GCMs, unifying the representation of both precipitating and non-precipitating clouds as well as the transition between them. These studies indicate a path to improve the representation of cloud lifetime effects in CAM5. Our future work will focus on improving the treatment of autoconversion in CAM5 and applying the S_{pop} metric to evaluate new model improvements in aerosol-cloud interactions.

Development of new diagnostics in CAM5 to quantify aerosol direct and indirect effects

Anthropogenic aerosols influence the energy balance of the Earth both directly, through scattering and absorbing sunlight, and indirectly, through their influence on the energy balance of clouds. The first mechanism, called direct radiative forcing, arises from contributions from several different aerosol components, such as sulfate, organic carbon, black carbon, mineral dust, and sea salt. To isolate the contribution of each aerosol component to the total direct radiative forcing, we worked with NCAR staff to augment the diagnostic radiation package in CAM5. The package allows one to perform an additional diagnostic radiation calculation with any set of radiatively active species (gas or aerosol) prescribed or simulated in CAM5. It produces separate values of energy balance variables for each diagnostic case. By differencing energy balance terms for pairs of different cases, one can determine the radiative impact of the set of species present in one case but missing in the other. To ensure that the radiative impact accounts for the influence of not only the species of interest but also the water associated with the species, the diagnosis recalculates both the dry and wet sizes of the set of species in each aerosol mode.

We used this new capability to make a more reliable estimate of the direct radiative forcing by anthropogenic sulfate, black carbon, organic carbon, mineral dust, and sea salt aerosol. These calculations form the basis for a *Journal of Climate* article (Ghan et al. 2012) that decomposes the anthropogenic aerosol radiative forcing simulated by CAM5. Interestingly, Ghan et al. found that the sum of the direct radiative forcing calculated for each aerosol component differs by 0.1 W m-2 from the direct radiative forcing by all components together.

4.0 Integration

In the final years of this project, we are increasingly focused on coupled applications of CESM to evaluate the impact of our improvements in the fully coupled system. We begin by describing our initial exploratory efforts in understanding the coupled system, and then follow with a discussion of next steps.

Baseline CMIP5 coupled simulations

We performed historical runs with CESM1 to evaluate the model performance and to understand the role of aerosols in fully coupled simulations. The output also has been processed in collaboration with NCAR and published through the Earth System Grid as part of the CMIP5 intercomparison project so that the scientific community can access our simulations. We briefly describe the new simulations in Hurrell (2012). Arctic sea ice change simulated by CESM1 is close to that observed (Figure 4.1), and we performed a number of transient climate simulations, "fixing" certain forcing agents (e.g., greenhouse gases, aerosols, etc.) to tease out the role of different forcing agents. Figure 4.2 shows the change in the top-of-atmosphere shortwave flux between pre-industrial and present-day climate due to various forcing agents and feedbacks, estimated through a careful differencing of these runs with extra diagnostics. The simulations demonstrate the rather small aerosol direct effect while aerosol indirect, semi-direct effects and various feedbacks are quite large in CESM1.

Yoon et al. (2012d) explored the role of anthropogenic aerosols from North America and Europe in influencing the multi-decadal variability of rainfall over the Sahel. The African Sahel has experienced unprecedented drought during the 1970s and 80s with modest signs of recovery in the 1990s. This long-term change in rainfall over land areas as large as the Sahel has been attributed to both natural variability such as the Atlantic Multi-decadal Oscillation and to anthropogenic causes, such as aggressive land management. Recent studies suggest anthropogenic aerosols from industrialized countries could play a role in the Sahel drought through cooling SST over the North Atlantic Ocean, favoring southward shift of the ITCZ and a reduced African monsoon. Our study with the CESM1 suggests that both the Sahel drought and recovery could be attributed to anthropogenic aerosols. Successful simulation of both the drought and subsequent recovery phases provides further evidence that anthropogenic aerosol emissions could be an important factor controlling rainfall variability over the Sahel.

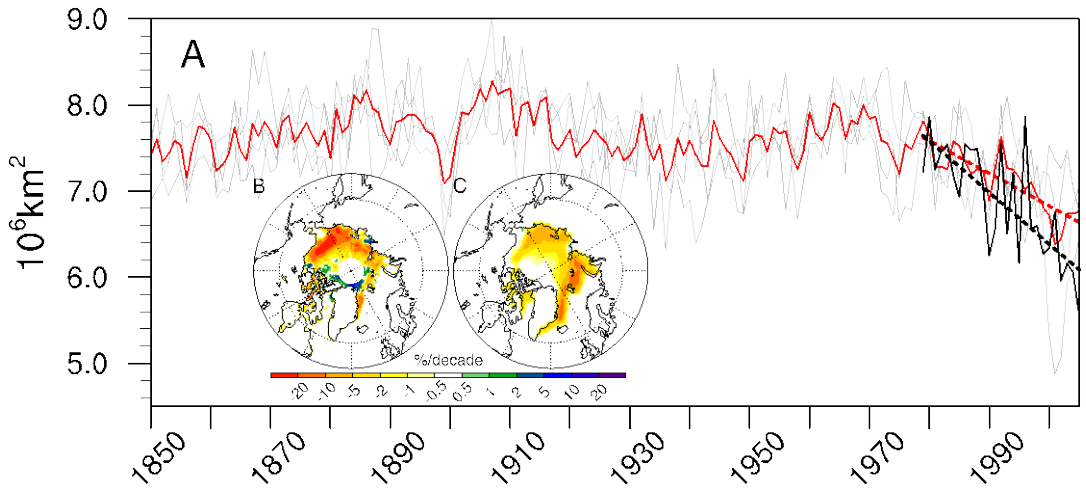

Figure 4.1. September Arctic Sea Ice Extent from satellite observation (black line) and the ensemble mean of historical runs of CESM1_POP (red line) with four individual members in thin grey lines (a) in the same manner as (Fetterer et al. 2009, from Yoon et al. 2012d). Linear trends of both observation and the ensemble mean during the period of 1979–2005 are marked as dashed lines. Spatial distribution of linear trend during the period of 1979–2005 based on satellite observation (b) and the ensemble mean of CESM1_POP simulations (c) described in Hurrell et al. (2012).

In S-Y Wang et al. (2012), we investigated how El Niño and Southern Oscillation (ENSO) change in the 20th century and whether there is evidence for an anthropogenic fingerprint on ENSO. Using multiple observational and modeling data sets, we document a strengthening relationship between boreal winter SST anomalies (SSTA) in the western North Pacific (WNP) and the development of the ENSO in the following year. The increased WNP-ENSO association emerged in the mid-20th century and has grown through the present, reaching correlation coefficients as high as ~0.7 in recent decades. Fully coupled CESM1 experiments replicate the WNP-ENSO association and indicate that greenhouse gases (GHG) are largely responsible for this observed increase. We hypothesize that shifts in the location of the largest positive SST trends between the subtropical and Tropical Western Pacific impacts the low-level circulation in a manner that reinforces the link between the WNP and the development of ENSO. A strengthened GHG-driven relationship between the WNP and ENSO provides an example of how anthropogenic climate change can directly influence, and potentially improve, the skill of intra-seasonal-to-inter-annual climate prediction. In S-Y Wang et al. (2012), we demonstrated how the relationship between ENSO and its precursor in WNP changes in the 20th century and how well that relationship is captured by CESM1 simulations.

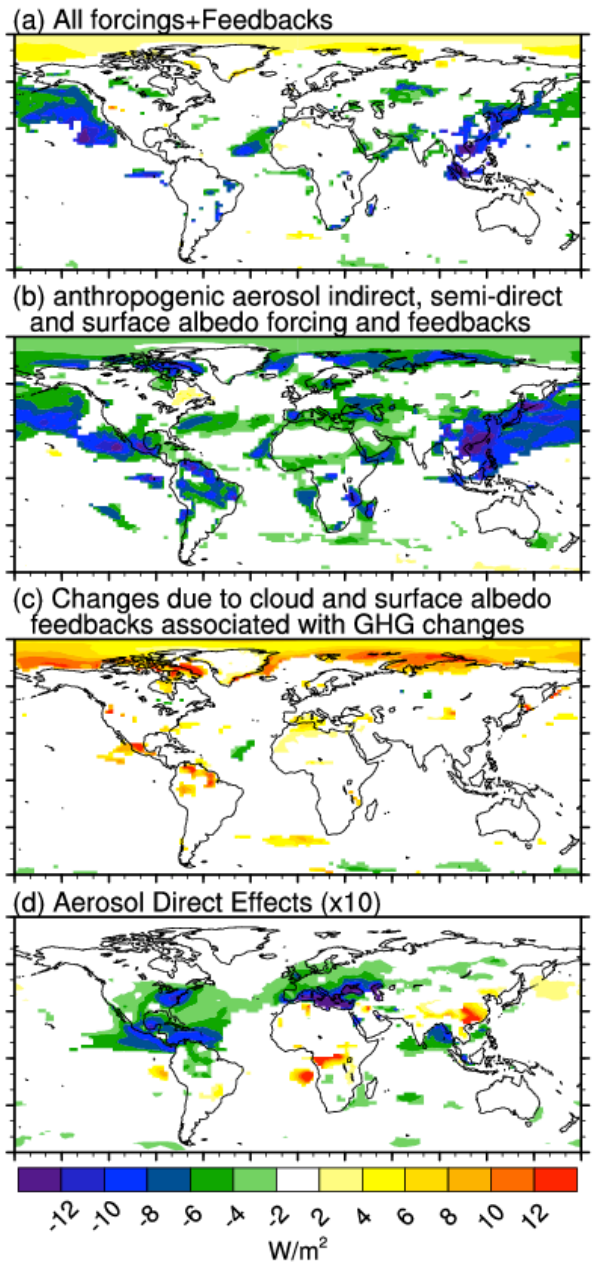

Figure 4.2. Panel (a) shows the flux changes associated with all forcings and feedbacks (estimated to occur from emission changes of aerosol and greenhouse gases and cloud, water vapor and surface albedo feedbacks calculated by differencing the first (1850-1859) and last (1996-2005) decade of the difference between AF and NASV). Panel (b) shows the anthropogenic aerosol indirect, semi-direct, and surface albedo forcing and feedbacks (produced from DRTNOAER for the TA run). Panel (c) shows the flux changes due to cloud and surface albedo feedbacks associated with greenhouse gas changes, calculated by differencing the fields in panels (a) and (b). Panel (d) shows the flux changes associated with the aerosol direct effect (calculated by first differencing the radiative fluxes calculated with tropospheric aerosols and without (DRTNOAER), and then differencing that quantity between the AF and NASV runs). Note the flux changes in (d) have been multiplied by 10. Areas without significant forcing at the 95% confidence level are white.

To help coordinate our efforts in understanding the coupled systems, we created three working groups each with a different focus.

4.1 Cloud and Aerosol Working Group

The first working group is focused on evaluating the cloud and aerosol processes of the Arctic climate system. Much of this work is on understanding and improving these processes in CAM5 and can be performed with simpler configurations (e.g., atmosphere with slab ocean).

4.1.1 Progress

Bi-weekly conference calls have allowed the group to familiarize ourselves with each other's work and have provided an effective support group for improving team members' individual research efforts. These meetings have brought team members together and sparked collaboration. As an example, Drs. Shaocheng Xie, Xiaohong Liu, Chuanfeng Zhao, and Yuying Zhang recently submitted a paper to the *Journal of Climate* (Xie et al. 2012) on the impact of changing the ice nucleation parameterization in CAM5. Dr. Xie led the project, calling on his experience in evaluation of climate models with observations and modeling testbeds. Dr. Liu brought ice parameterization experience, and Drs. Zhang and Zhao provided satellite simulator and ARM measurement experience to the project. Comparison against ARM observations shows the new scheme clearly improves cloud properties, leading to a reduction in surface radiation error. Use of satellite simulators reveals that improvement is due to better simulation of low clouds; mid- and upper-level clouds become too optically thick under the new ice nucleation scheme.

A major goal of this sub-group over the past year has been to develop the infrastructure needed for unified model development efforts across labs. To this end, we have merged PNNL and LLNL CAM5 model changes into a single code base derived from the very recent cam5_1_31 tag. This allows us to make use of single column and COSP capabilities not yet available in the public release as well as to ensure that our model changes don't conflict with each other. A common tag is also critical for planned coupled-model simulations to be performed by PNNL at NERSC. Merging has not yet yielded the synergistic improvement we had hoped for. We are actively working on this issue.

Another goal of this group is to develop synergy between model development and model diagnostic components of the project. Too often, diagnostic projects focus on old model versions that are not relevant to current development directions. Similarly, model development often focuses on too narrow a set of metrics, leading to surprises later in the development cycle or upon release. We seek to avoid these issues by routinely including development versions of the model in our diagnostic analyses. To this end, we have developed the ability to share model data across laboratories via the Earth System Grid Federation (ESGF) framework. We also routinely post figures from NCAR's Atmospheric Model Working Group (AMWG) diagnostics package at a centralized location (climate.pnnl.gov). Standardized run and output configuration also aids analysis. Finally, we have identified contact people responsible for performing various analyses on development versions of the code. Because of development-cycle timing, this effort is just now beginning to bear fruit.

4.1.2 Plans

Our goal for next year is to improve our understanding of the impact our combined model changes have made, using the infrastructure we have created that connects model development and diagnostic efforts. This will guide future model development and diagnostic strategies. We will also perform coupled simulations to assess the impact of our changes in CESM. The Interactions Working Group (section 4.2) will start to evaluate how the model developments impact the model's ability to predict Arctic climate and sea ice change.

4.2 Biogeochemistry Working Group

The biogeochemistry working group will be integrating the biogeochemical improvements across components to evaluate complete element cycling throughout the system.

4.2.1 Progress

Initial discussions and conference calls on the surface exchange of organics have resulted in initial interactions between Dr. Scott Elliott (LANL) and PNNL researchers. Dr. Elliott generated some initial estimates of surface fluxes using some simple approaches. A new SciDAC project, Applying Computationally Efficient Schemes for BioGeoChemical Cycles (ACES4BGC), will attend to some aspects of biogeochemical modeling, but work will continue on this project on components of the BGC relevance to cloud-aerosol interactions.

4.2.2 Plans

As discussed previously, a scheme being implemented in CICE will simulate vertical transport of nutrients and other important species through the ice, as well as biogeochemical processing within the sea ice. Results will need to be validated against observations from atmosphere aerosol data sets, and forcing data sets for initial validation simulations will need to be developed.

4.3 Interactions Working Group

The Interactions Working Group has two main goals: (1) to integrate and evaluate the sea ice and ocean improvements described in previous sections, and (2) develop diagnostic frameworks to test CESM's interactions between modeling components. This final working group is meant to integrate across all components for the evaluation of all improvements in the fully coupled system.

4.3.1 Progress

While the ice and ocean improvements are not yet ready for evaluation in the fully coupled model, some progress has been made in model coupling, diagnostic development, and baseline simulations.

Model Coupling: Recently, members of this project jointly organized a workshop on polar boundary layer processes, including ocean, ice and atmosphere interfaces (Hunke and Meier 2012). A number of project participants attended or contributed to this highly successful workshop.

As part of the original proposal for this project, we described some outstanding ocean/ice coupling issues. We have made some moderate fixes to this coupling, mostly involving the time consistency of the dynamical terms and these have made a small improvement around the ice edge. However, our experience with high-resolution coupled simulations has uncovered instability in the ice/ocean momentum flux calculation that results in rapid acceleration of both ocean and ice. Similar instability has also been identified in other high-resolution simulations and even at coarse resolution (Dr. Frank Bryan, private communication). Reducing the coupling frequency can mitigate the impact of this instability, but the cause has not yet been determined, and we continue to explore this issue. Finally, we have begun to implement a new vertical coordinate scheme in the POP ocean model that will better enable the implementation of realistic ocean-ice coupling formulations.

Diagnostic frameworks: Diagnostics of the interactions between modeling components has focused on the response of low-level Arctic clouds to Arctic surface type, and understanding the controls of 20th century Arctic sea ice loss. The response of Arctic low-level clouds to surface type is dependent on atmospheric thermodynamics (Barton et al. 2012). When going from a sea ice covered surface to open ocean, cloud amount increases at the lowest atmospheric levels when the lower troposphere is very stable. When the lower atmosphere is less stable, the Arctic cloud amount at the lowest levels decrease when they occur over open water compared to over sea ice. In understanding the controls of 20th century Arctic sea ice loss, Yoon et al. (2012) examined SOM output with different atmospheric forcings (e.g., aerosols, CO_2). Yoon et al. (2012) found that ocean heat transport is a key process in reducing Arctic sea ice cover.

4.3.2 Plans

Future research in the Interactions Working Group will focus on evaluating parameterization updates in CICE, and on importing the sea ice and ocean parameterization updates into CESM. The merging of CICE improvements is expected to be complete by the end of CY2012 and a new CICE release is planned for mid-2013, but simulations to evaluate these changes can be started in early 2013.

CESM coupled-model runs, with changes to the CAM code, will be performed in early 2013. The interactions group will analyze these model runs with a focus on understanding the differences in the forecast, AMIP, and fully coupled runs. Specific research areas include understanding the role of Arctic clouds on the surface radiative budget and variability in sea ice concentration.

5.0 Conclusions and Future Work

In an effort to improve our model representation and understanding of high-latitude climate change, our project has made substantial progress on many fronts. The work has spanned all components of the CESM. We have begun to integrate these changes into the released version of the CESM and to evaluate the improvements in partially coupled tests. We will soon perform fully coupled climate change simulations. This change in focus requires more communication and joint work among our team, and we created a new working group structure to help integrate and coordinate these efforts.

6.0 Project Publications

The following are peer-reviewed publications resulting from the work under this project during the current reporting period. Publications that are in preparation, submitted, in review, or in revision are shaded in grey. Many other oral presentations and posters have been given at program meetings, CESM workshops and working group meetings, and scientific conferences like the American Geophysical Union and other more specific meetings.

Anderson BT, C Deser, AS Phillips, JR Knight, MA Ringer, JH Yoon, and A Cherchi. 2012. Testing for the possible influence of unknown climate forcings upon global temperature increases from 1950-2000. *Journal of Climate*, doi:10.1175/JCLI-D-11-0064.

Barton NP, S Klein, and J Boyle. 2012. "Arctic synoptic regimes: Comparing domain wide Arctic cloud observations with CAM4 and CAM5 during similar dynamics." *Journal of Geophysical Research* 117:D15205, doi:10.1029/2012D017589.

Barton NP, S Klein, and J Boyle. 2013. "An analysis of Arctic lower tropospheric stability in global climate models." *Journal of Climate*. In preparation.

Caldwell PM, S Park, and S Klein. 2012a. "Improving cloud process interactions in a global climate model." *Geophysical Model Development*. In preparation.

Caldwell PM, H Morrison, S Klein, H Wang, and P Rasch. 2012b. "The case of the missing condensate – the importance of thinking about process coupling." *Geophysical Model Development*. In preparation.

Chand D, R Wood, SJ Ghan, M Wang, M Ovchinnikov, PJ Rasch, S Miller, B Schichtel, and T Moore. 2012. "Aerosol optical depth increase in partly cloudy conditions." *Journal of Geophysical Research* 117:D17207, doi:10.1029/2012JD017894.

Chen CC and PJ Rasch. 2011. "Climate simulations with an isentropic finite-volume dynamical core." *Journal of Climate* 25:2843-2861, doi:dx.doi.org/10.1175/2011JCLI4184.1.

Chen M, JC Rowland, CJ Wilson, GL Altmann, and SP Brumby. 2012a. "Temporal and Spatial Pattern of Thermokarst Lake Area Changes at Yukon Flats, Alaska." *Hydrological Processes*. In press.

Chen M, JC Rowland, CJ Wilson, GL Altmann, and SP Brumby. 2012b. "Understanding intra-annual and inter-annual lake area change dynamics in Yukon Flats, Alaska, Permafrost and Periglacial Processes." In review.

de Boer G, WD Collins, S Menon, and CN Long. 2011. "Using Surface Remote Sensors to Derive Radiative Characteristics of Mixed-Phase Clouds: An example from M-PACE." *Atmospheric Chemistry Physics* 11:11937-11949, doi:10.5194/acp-11-11937-2011.

Deal C, N Steiner, J Christian, J Clement-Kinney, K Denman, S Elliott, G Gibson, M Jin, D Lavoie, S Lee, W Lee, W Maslowski, J Wang, and E Watanabe. 2012. "Progress and challenges in biogeochemical modeling of the Pacific Arctic." Chapter 12 in *The Pacific Arctic Region Post-IPY Synthesis: Status, Trends and Climate Warming,* ed. J Grebmaier, Springer Verlag.

Elliott S, C Deal, G Humphries, E Hunke, N Jeffery, M Jin, M Levasseur, and J Stefels. 2012. "Pan-Arctic simulation of coupled nutrient-sulfur cycling due to sea ice biology." *Journal of Geophysical Research–Biogeosciences* 117:G01016.

Flocco D, D Schroeder, DL Feltham, and EC Hunke. 2012. "Impact of melt ponds on Arctic sea ice simulations from 1990 to 2007." *Journal of Geophysical Research*, doi:10.1029/2012JC008195.

Frost GJ, S Falke, C Granier, T Keating, JF Lamarque, M Melamed, P Middleton, G Petron, and SJ Smith. 2012. "New Directions: Toward a community emissions approach." *Atmospheric Environment* 51:333-334. doi:10.1016/j.atmosenv.2012.01.055.

Ganguly D, PJ Rasch, H Wang, and J-H Yoon. 2012a. "Climate response of the South Asian monsoon system to anthropogenic aerosols." *Journal of Geophysical Research* 117:D13209, doi:10.1029/2012JD017508.

Ganguly D, PJ Rasch, H Wang, and J-H Yoon. 2012b. "Fast and slow responses of the South Asian monsoon system to anthropogenic aerosols." *Geophysical Research Letters*, doi:10.1029/2012GL053043.

Gantt B, J Xu, N Meskhidze, Y Zhang, A Nenes, SJ Ghan, X Liu, R Easter, and R Zaveri. 2012. "Global distribution and climate forcing of marine organic aerosol - Part 2: Effects on cloud properties and radiative forcing." *Atmospheric Chemistry Physics* 12:7453-7474.

Gent PR, LJ Donner, MM Holland, EC Hunke, SR Jayne, DM Lawrence, RB Neale, PJ Rasch, M Vertenstein, PH Worley, Z-L Yang, and M Zhang. 2011. "The Community Climate System Model Version 4." *Journal of Climate* 24(19):4973-4991, doi: 10.1175/2011JCLI4083.1.

Ghan SJ, H Abdul-Razzak, A Nenes, Y Ming, X Liu, M Ovchinnikov, B Shipway, N Meskhidze, J Xu, and X Shi. 2011. "Droplet nucleation: physically based parameterizations and comparative evaluation." *Journal of Advances in Modeling Earth Systems* 3:M10001, doi:10.1029/2011MS000074.

Ghan SJ, X Liu, RC Easter, R Zaveri, PJ Rasch, J-H Yoon, and B Eaton. 2012. "Toward a minimal representation of aerosols in climate models: Comparative decomposition of aerosol direct, semi-direct and indirect radiative forcing." *Journal of Climate* 25:6461-6476, doi: 10.1175/JCLI-D-11-00650.1.

Humphries G, C Deal, S Elliott, and F Huettmann. 2012. "Spatial predictions of sea surface dimethylsulfide concentrations in the high Arctic using physical ocean characteristics." *Biogeochemistry*, doi:10.1007/s10533-011-9683-y.

Hunke EC, DA Herbert, and O Lecomte. 2012. "Level-ice melt ponds in the Los Alamos Sea Ice Model, CICE." *Ocean Modelling*. In revision.

Hunke EC and W Meier. 2012. "Polar boundary layer processes: Important factors for investigating biogeochemistry and climate, EOS meeting report from the workshop Ice at the Interface." *Atmosphere-Ice-Ocean Boundary Layer Processes and Their Role in Polar Change*, June 25-27, 2012, Boulder, Colorado USA. In press.

Hurrell JW, MM Holland, S Ghan, J-F Lamarque, D Lawrence, WH Lipsbcomb, N Mahowald, D March, P Rasch, D Bader, WD Collins, RR Gent, JJ Hack, J Kiehl, P Kushners, WG Large, S Marshall, S Vavrus, and M Vertenstein. 2012. "The Community Earth System Model: A framework for collaborative research. Submitted to *BAMS*.

Jeffery N, E Hunke, and AK Turner. 2012. "The CICE sea ice model with prognostic salinity: Arctic simulations." *Journal of Geophysical Research*. Submitted.

Jeffery N, E Hunke, and SM Elliott. 2011. "Modeling the transport of passive tracers in sea ice." *Journal of Geophysical Research* 116:C07020, doi:10.1029/2010JC006527.

Jin M, C Deal, S Elliott, E Hunke, M Maltrud, and N Jeffery. 2012. "Sea ice and ocean primary production in a global ecosystem model." *Deep-Sea Research*. In press.

Kay JE, B Hillman, S Klein, Y Zhang, B Medeiros, G Gettelman, R Pincus, B Eaton, J Boyle, R Marchand, and T Ackerman. 2012. "Exposing global cloud biases in the Community Atmosphere Model (CAM) using satellite observations and their corresponding instrument simulators." *Journal of Climate* 25:5190-5207, doi: 10.1175/JCLI-D-11-00469.1.

Klein S, Y Zhang, M Zelinka, J Boyle, P Gleckler, and R Pincus. 2012. "Are climate model simulations of clouds improving? An evaluation using the ISCCP simulator." *Journal of Geophysical Research*. In revision.

Lamarque J-F, LK Emmons, PG Hess, DE Kinnison, S Tilmes, F Vitt, CL Heald, EA Holland, PH Lauritzen, J Neu, JJ Orlando, PJ Rasch, and G Tyndall. 2012. "CAM-Chem: description and evaluation of interactive atmospheric chemistry in the Community Earth System Model." *Geophysical Model Development* 5:369-411, doi:10.5194/gmd-5-369-2012.

Lee Y, M Flanner, C Jiao, J-F Lamarque, D Shindell, G Faluvegi, M Bisiaux, J Cao, WJ Collins, M Curran, S Dalsoren, S Doherty, R Edwards, S Ghan, J McConnell, G Myhre, T Nagashima, V Naik, S Rumbold, R Skeie, K Sudo, T Takemura, and F Thevenon. 2012. "Evaluation of pre-industrial to present-day black carbon aerosols and its albedo forcing from ACCMIP (Atmospheric Chemistry and Climate Model Intercomparison Project)." *Atmospheric Chemistry Physics*. Submitted.

Liu X, RC Easter, SJ Ghan, R Zaveri, P Rasch, X Shi, J-F Lamarque, A Gettelman, H Morrison, F Vitt, A Conley, S Park, R Neale, C Hannay, A Ekman, P Hess, N Mahowald, W Collins, M Iacono, C Bretherton, M Flanner, and D Mitchell. 2012. "Toward a minimal representation of aerosols in climate models: Description and evaluation in the Community Atmosphere Model CAM5." *Geoscientific Model Development* 5:709-739, doi:10.5194/gmd-5-709-2012.

Liu X, S Xie, J Boyle, SA Klein, X Shi, Z Wang, W Lin, SJ Ghan, M Earle, PSK Liu, and Z Wang. 2011. "Testing cloud microphysics parameterizations in NCAR CAM5 with ISDAC and M-PACE observations." *Journal of Geophysical Research* 116:D00T11, doi:10.1029/2011JD015889.

Loose B, L Miller, S Elliott, and T Papakyriakou. 2011. "Sea ice biogeochemistry with transfer of CO_2 and other gases." *Oceanography* 24: 202-218.

Ma P-L, PJ Rasch, H Wang, S Tilmes, X Liu, J-F Lamarque, J Fast, DM Winker. 2012a. "Uncertainties of aerosol transport into the Arctic associated with simulated meteorological fields." *Journal of Geophysical Research*. Submitted.

Ma P-L, et al. 2012b. "Evaluating the CAM5 physics suite within a regional model: Bringing the regional and global modeling communities together." In preparation.

Ma P-L, et al. 2012c. "The resolution dependency of CAM5 physics suit and its ramification on aerosol transport into the Arctic." In preparation.

Ma P-L, K Zhang, JJ Shi, T Matsui, and A Arking. 2011. "Direct radiative effect of mineral dust on the development of African easterly waves in late summer, 2003-2007." *Journal of Applied Meteorology and Climatology,* doi:10.1175/JAMC-D-11-0215.1. In press.

Meskhidze N, J Xu, B Gantt, Y Zhang, A Nenes, SJ Ghan, X Liu, R Easter, and R Zaveri. 2011. "Global distribution and climate forcing of marine carbonaceous aerosol. 1. Model improvements and evaluation." *Atmospheric Chemistry Physics* 11:11689-11705, doi:10.5194/acp-11-11689-2011.

Myhre G, BH Samset, RB Skeie, TK Berntsen, H Zhang, Z Wang, A Kirkevåg, T Iversen, Ø Seland, SJ Ghan, X Liu, RC Easter, PJ Rasch, J-H Yoon, F Yu, G Luo, X Ma, S Bauer, K Tsigaridis, H Bian, SD Steenrod, T Diehl, M Chin, G Lin, J Penner, Y Balkanski, M Schulz, D Hauglustaine, N Bellouin, K Zhang, P Stier, J-F Lamarque, T Takemura, and S Kinne. 2012. "Radiative forcing of the direct aerosol effect from AeroCom Phase II simulations." *Atmospheric Chemistry Physics.* Submitted.

Petersen M, S Williams, M Maltrud, M Hecht, and B Hamann. 2012. "A three-dimensional eddy census of a high-resolution global ocean simulation." *Journal of Geophysical Research*. Submitted.

Popova E, A Yool, A Coward, F Dupont, C Deal, S Elliott, E Hunke, M Jin, M Steele, and J Zhang. 2012. "Factors controlling Arctic Ocean primary production in coupled physical-biological models." *Journal of Geophysical Research–Biogeosciences* 117, doi:10.1029/2011JC007112.

Rasch PJ and co-Authors. 2012. "A description of the Community Atmosphere Model (Version 5)." *Journal of Climate*. In Preparation.

Rosenfeld D, H Wang, and PJ Rasch. 2012. "The roles of cloud drop effective radius and LWP in determining rain properties in marine stratocumulus." *Geophysical Research Letters* 39:L13801, doi:10.1029/2012GL052028.

Sednev I and S Menon. 2012. "Analyzing numerics of bulk microphysics schemes in community models: warm rain processes." *Geoscientific Model Development* 5:975-987, doi:10.5194/gmd-5-975-2012.

Shindell DT, J-F Lamarque, M Schulz, M Flanner, C Jiao, M Chin, P Young, Y Lee, L Rotstayn, G Milly, G Faluvegi, Y Balkanski, W Collins, AJ Conley, S Dalsoren, R Easter, S Ghan, L Horowitz, X Liu, G Myhre, T Nagashima, V Naik, S Rumbold, R Skeie, K Sudo, S Szopa, T Takemura, A Voulgarakis and J-H Yoon. 2012. "Radiative forcing in the ACCMIP historical and future climate simulations." *Atmospheric Chemistry Physics*. Submitted.

Smith SJ, J van Aardenne, Z Klimont, R Andres, AC Volke, and S Delgado Arias. 2011. "Anthropogenic sulfur dioxide emissions: 1850-2005." *Atmospheric Chemistry and Physics* 11(3):1101-1116. doi:10.5194/acp-11-1101-2011.

Turner AK, EC Hunke, and CM Bitz. 2012. "Two modes of sea-ice gravity drainage." *Journal of Geophysical Research*. Submitted.

Vinoj V, PJ Rasch, H Wang, J-H Yoon, and P-L Ma. 2012. "A dusty western Asian link to Indian summer monsoon rainfall." *Nature Geosciences*. Submitted.

Wang H, R Easter, P Rasch, M Wang, X Liu, S Ghan, Y Qian, J-H Yoon, P-L Ma, and V Vinoj. 2012a. "Sensitivity of remote aerosol distributions to representation of cloud-aerosol interactions in a global climate model." *Geoscientific Model Development*. Submitted.

Wang H. et al. 2012b. "Impact of increased absorbing aerosols in the Arctic on snow and sea ice in CAM5." In preparation.

Wang H, PJ Rasch, RC Easter, N Beagley, and B Singh. 2012c. "CAM5 Estimates of Global Source-Receptor Relationships for Black Carbon under Present-day Emission Scenario." In preparation.

Wang M, S Ghan, M Ovchinnikov, X Liu, R Easter, E Kassianov, Y Qian, and H Morrison. 2011. "Aerosol indirect effects in a multi-scale aerosol-climate model PNNL-MMF." *Atmospheric Chemistry and Physics* 11:5431-5455, doi:10.5194/acp-11-5431-2011.

Wang M, SJ Ghan, X Liu, T L' Ecuyer, K Zhang, H Morrison, M Ovchinnikov, RC Easter, RT Marchand, D Chand, Y Qian, and JE Penner. 2012. "Constraining cloud lifetime effects of aerosols using A-Train Satellite observations." *Geophysical Research Letters* 39:L15709, doi:10.1029/2012GL053111.

Wang S-Y, M L'Heureux, and J-H Yoon. 2012. "Are greenhouse gases changing ENSO precursors in the Western North Pacific?" *Journal of Climate*. In revision.

Wingate B, P Embid, M Holmes-Cerfon, and M Taylor. 2011. "Low Rossby limiting dynamics for stably stratified flow with finite Froude number." *Journal of Fluid Mechanics*, doi:10.1017/jfm.2011.69.

Xie S, X Liu, C Zhao, and Y Zhang. 2012. "Sensitivity of CAM5 simulated Arctic clouds and radiation to ice nucleation." *Journal of Climate*. Under revision.

Yang B, Y Qian, G Lin, LR Leung, PJ Rasch, GJ Zhang, SA McFarlane, C Zhao, Y Zhang, H Wang, M Wang, and X Liu. 2012. "Uncertainty quantification and parameter tuning in the CAM5 Zhang-McFarlane convection scheme and physical impact of improved convection on the global circulation and climate." *Journal of Geophysical Research*. Submitted.

Yoon J-H, PJ Rasch, K Balaguru, C Hannay, and B Singh. 2012a. "The role of the oceanic heat transport on Arctic sea ice change in the 20th century." Submitted.

Yoon J-H, PJ Rasch, S Ghan et al. 2012b. "Climate Sensitivity in the presence of Aerosols: Prescribing aerosol direct and indirect effects." In preparation.

Yoon J-H, PJ Rasch, H Wang, V Velu, and D Ganguly. 2011c. "Impacts of carbonaceous aerosol on hydrological cycle over the Northern Africa." *Geophysical Research Letters*. Submitted.

Yoon J-H, PJ Rasch, S Hagos, B Singh, V Vinoj, S-Y Wang, and N Zeng. 2012d. "Sahel drought and recovery in the 20th century: Aerosol as a pace maker." Submitted.

Zhang Y, S Xie, C Covey, DD Lucas, P Gleckler, S Klein, J Tannahill, C Doutriaux, and R Klein. 2012. "Regional assessment of the parameter-dependent performance of CAM4 in simulating tropical clouds." *Geophysical Research Letters* 39:L14708, doi:10.1029/2012GL052184.

Zhao C, SA Klein, S Xie, X Liu, JS Boyle, and Y Zhang. 2012. "Aerosol first indirect effects on non-precipitating low-level liquid cloud properties as simulated by CAM5 at ARM sites." *Geophysical Research Letters* 39:L08806, doi:10.1029/2012GL051213.

7.0 Other References

Boe J, A Hall, and X Qu. 2009. "Current GCMs' unrealistic negative feedback in the Arctic." *Journal of Climate* 22:4682-4695.

Cavalieri D, C Parkinson, P Gloersen, and HJ Zwally. 1996. "Sea ice concentrations from Nimbus-7 SMMR and DMSP SSMI/I-SSMIS passive microwave data [1981-1992]." National Snow and Ice Data Center, digital media, ftp://sidads.colorado.edu/DATASETS/NOAA/G02135/north/daily/data/, updated yearly.

Claquin T, M Schulz, and YJ Balkanski. 1999. "Modeling the mineralogy of atmospheric dust sources." *Journal of Geophysical Research* 104:22243-22256.

Flanner MG, X Liu, C Zhou, JE Penner, and C Jiao. 2012. "Enhanced solar energy absorption by internally mixed black carbon in snow grains." *Atmospheric Chemistry and Physics* 12(10):4699-4721. doi:10.5194/acp-12- 4699-2012.

Hoose C, U Lohmann, R Erdin, and I Tegen. 2008. "The global influence of dust mineralogical composition on heterogeneous ice nucleation in mixed-phase clouds." *Environmental Research Letters* 3:025003, doi:10.1088/1748-9326/3/2/025003.

Kay JE and A Gettelman. 2009. "Cloud influence on and response to seasonal Arctic sea ice loss." *Journal of Geophysical Research* 114:D18204, doi:10.1029/2009JD0117733.

Kelly JT and AS Wexler. 2005. "Thermodynamics of carbonates and hydrates related to heterogeneous reactions involving mineral aerosol." *Journal of Geophysical Research* 110:D11201, doi: 10.1029/2004JD005583.

Kelly JT, CC Chuang, and AS Wexler. 2007. "Influence of dust composition on cloud droplet formation." *Atmospheric Environ*ment 41:2904-2916.

Kirchstetter TW, T Novakov, and PV Hobbs. 2004. "Evidence that the spectral dependence of light absorption by aerosols is affected by organic carbon." *Journal of Geophysical Research* 109:D21208, doi:10.1029/2004JD004999.

D Koch, M Schulz, S Kinne, C McNaughton, JR Spackman, Y Balkanski, S Bauer, T Berntsen, TC Bond, O Boucher, M Chin, A Clarke, N De Luca, F Dentener, T Diehl, O Dubovik, R Easter, DW Fahey, J Feichter, D Fillmore, S Freitag, S Ghan, P Ginoux, S Gong, L Horowitz, T Iversen, A Kirkevåg, Z Klimont, Y Kondo M Krol, X Liu, R Miller, V Montanaro, N Moteki, G Myhre, JE Penner, J Perlwitz, G Pitari, S Reddy, L Sahu, H Sakamoto, G Schuster, JP Schwarz, Ø Seland, P Stier, N Takegawa T Takemura, C Textor, JA van Aardenne, and Y Zhao. 2009. "Evaluation of black carbon estimations in global aerosol models." *Atmospheric Chemistry and Physics* 9:9001-9026, doi:10.5194/acp-9-9001-2009.

Liu X and J Wang. 2010. "How important is organic aerosol hygroscopicity to aerosol indirect forcing?" *Environmental Research Letters* 5:044010, doi: 10.1088/1748- 9326/5/4/044010.

Lohmann U and K Diehl. 2006. "Sensitivity studies of the importance of dust ice nuclei for the indirect aerosol effect on stratiform mixed-phase clouds." *Journal of the Atmospheric Sciences* 63(3): 968-982.

Liu X and J Wang. 2010. "How important is organic aerosol hygroscopicity to aerosol indirect forcing?" *Environmental Research Letters* 5:044010, doi: 10.1088/1748- 9326/5/4/044010.

Maltrud M, F Bryan, M Hecht, E Hunke, D Ivanova, J McClean, and S Peacock. 2008. "Global ocean modelling in the eddying regime using POP." *CLIVAR Exchanges* 44:5-8.

Maltrud M, F Bryan, and S Peacock. 2010. "Boundary impulse response functions in a century-long eddying global ocean simulation." *Environmental Fluid Mechanics* 10:275-295, doi: 10.1007/s10652-009-9154-3.

McClean JL, DC Bader, FO Bryan, ME Maltrud, JM Dennis, AA Mirin, PW Jones, YY Kim, DP Ivanova, M Vertenstein, JS Boyle, RL Jacob, N Norton, A Craig, and PH Worley. 2011. "A prototype two-decade fully-coupled fine-resolution CCSM simulation." *Ocean Modelling* 39:10-30, doi:10.1016/j.ocemod.2011.02.011.

Medeiros B, C Deser, RA Tomas, and JE Kay. 2011. "Arctic inversion strength in climate models." *Journal of Climate* 24:4733-4740.

Meyers MP, PJ DeMott, and WR Cotton. 1992. "New primary ice-nucleation parameterization in an explicit cloud model." *Journal of Applied Meteorology* 31(7):708–721.

Notz D and MG Worster. 2008. "In situ measurements of the evolution of young sea ice." *Journal of Geophysical Research* 113:C03001, doi:10.1029/2007JC004333.

Palm SP, ST Strey, J Spinhirne, and T Markus. 2010. "Influence of Arctic sea ice extent on polar cloud fraction and vertical structure and implications for regional climate." *Journal of Geophysical Research* 115:D21209, doi:10.1029/2010JD013900.

Schweiger AJ, RW Lindsay, S Vavrus, and JA Francis. 2008. "Relationships between Arctic sea ice and clouds during autumn." *Journal of Climate* 21(18):4799-4810, doi:10.1175/2008JCLI2156.1.

Wang M, S Ghan, R Easter, M Ovchinnikov, X Liu, E Kassianov, Y Qian, WI Gustafson Jr., VE Larson, DP Schanen, M Khairoutdinov, and H Morrison. 2011a. "The multi-scale aerosol-climate model PNNL-MMF: model description and evaluation." *Geoscientific Model Development* 4(1):137-168.

Williams S, M Hecht, M Petersen, R Strelitz, M Maltrud, J Ahrens, M Hlawitschka, and B Hamann. 2011b. "Visualization and analysis of eddies in a global ocean simulation." *Computer Graphics Forum* 30:991-1000.

Williams S, J Ahrens, T Bremer, B Hamann, M Hecht, M Hlawitschka, and M Petersen. 2011b. "Adaptive extraction and quantification of discrete vortices." *IEEE Transactions on Visualization and Computer Graphics* 17:2088-2095.

Weijer W, ME Maltrud, MW Hecht, HA Dijkstra, and MA Kliphuis. 2012. "Response of the Atlantic Ocean Circulation to Greenland Ice Sheet Melting in a Strongly Eddying Ocean Model." *Geophysical Research Letters* 39, doi:10.1029/2012GL051611.

U.S. DEPARTMENT OF
ENERGY

Office of Science